



ENSO-based outlook of droughts and agricultural outcomes in Afghanistan

Shraddhanand Shukla^{a,*}, Fahim Zaheer^a, Andrew Hoell^b, Weston Anderson^{c,d},
Harikishan Jayanthi^e, Greg Husak^a, Donghoon Lee^{a,i}, Brian Barker^f, Shahriar Pervez^g,
Kimberly Slinski^{c,d}, Christina Justice^f, James Rowland^g, Amy L. McNally^d, Michael Budde^g,
James Verdin^h

^a Climate Hazards Center, University of California-Santa Barbara, Santa Barbara, CA, United States

^b Physical Sciences Laboratory, National Oceanic and Atmospheric Administration, 80305, Boulder, CO, United States

^c Earth System Science Interdisciplinary Center, University of Maryland, College Park, MD, United States

^d NASA Goddard Space Flight Center, Greenbelt, MD, United States

^e Arctic Slope Regional Corporation Federal Data Solutions, Contractor to U.S. Geological Survey, Earth Resources Observation and Science (EROS) Center, 57198, Sioux Falls, SD, United States

^f Department of Geographical Sciences, University of Maryland, College Park, MD, United States

^g U.S. Geological Survey, EROS Center, 57198, Sioux Falls, SD, United States

^h U.S. Agency for International Development, 20523, Washington, DC, United States

ⁱ Department of Civil Engineering, University of Manitoba, Winnipeg, MB, Canada

ABSTRACT

Drought is one of the key drivers of food insecurity in Afghanistan, which is among the most food insecure countries in the world. In this study, we build on previous research and seek to answer the central question: “What is the influence of El Niño-Southern Oscillation (ENSO) on drought outlooks and agricultural yield outcome in Afghanistan, and how do these influences vary spatially?” We do so by utilizing multiple indicators of droughts and available wheat yield reports. We find a clear distinction in the probability of drought (defined as being in the lower tercile) in Afghanistan during La Niña compared to El Niño events since 1981. The probability of drought in Afghanistan increased during La Niña, particularly in the North, Northeast, and West regions. La Niña events are related to an increase in the probability of snow drought, particularly in parts of the Amu Darya basin. It is found that relative to El Niño events, snow water equivalent [total runoff] during La Niña events January–March (March–July total runoff) decreases between 9% and 30% (28%–42%) for the five major basins in the country. The probability of agricultural drought during La Niña events is found to be higher than 70% in the rainfed and irrigated areas of the Northeast, North, and West regions. This result is at least partly supported by reported wheat yield composites related to La Niña events that tend to be lower than for El Niño events across all regions in the case of rainfed wheat (statistically significant in Northeast, West, and South regions) and in some cases for irrigated wheat. The results of this study have direct implications for improving early warning of worsening food insecurity in Afghanistan during La Niña events, given that we now have long-lead and skillful forecasts of ENSO up to 18–24 months in advance, which could potentially be used to provide earlier warning of worsening food insecurity in Afghanistan

1. Introduction

Irrigated and rainfed agriculture is central to the economy and food security of Afghanistan and a primary source of livelihood, food and income in rural areas. Water supply for irrigation is mainly supported by rivers and springs, driven by snowmelt (Rout 2008) with increasing contribution of groundwater in recent years, particularly in the Helmand basin (Nazemosadat et al., 2023). Winter precipitation, which typically spans from October to March (Fig. S1), is critical for snowfed water resources that support irrigated agriculture. Spring precipitation, which typically occurs between March to May (Fig. S1), supports rainfed agriculture. Fig. 1 shows the mean production of irrigated and rainfed

wheat in different sub-regions indicating that irrigated wheat makes up a larger portion of total wheat production in the country. Primary irrigated wheat production regions are the Northeast, North, East, South, and Southwest sub-regions, and primary rainfed wheat production regions are Northeast, North, and West sub-regions (Fig. 1)

Despite agriculture being the backbone of the economy, Afghanistan is still one of the most food insecure countries in the world. As per the 2022 Global Hunger Index (GHI), Afghanistan, as of October 2022, has a GHI of 29.9, which falls in the “serious” category (GHI 2022), and ranks amongst the lowest (109th) out of the 121 countries for which 2022 GHI scores were calculated. The GHI is a collective measure of several malnutrition related indicators such as Undernourishment, Child

* Corresponding author.

E-mail address: sshukla@ucsb.edu (S. Shukla).

<https://doi.org/10.1016/j.wace.2024.100697>

Received 20 July 2023; Received in revised form 23 May 2024; Accepted 24 May 2024

Available online 28 May 2024

2212-0947/© 2024 The Authors. Published by Elsevier B.V. This is an open access article under the CC BY-NC license (<http://creativecommons.org/licenses/by-nc/4.0/>).

stunting, Child wasting, and Child mortality (Wiesmann et al., 2015)

In addition to the longer-term context above, presently, the country is facing an unprecedented food insecurity related humanitarian crisis. Based on 2023 estimates, about two-thirds of the population will need urgent humanitarian assistance (OCHA 2023). Drought is one of the key drivers (FEWS NET 2023; IPC 2022) of this unprecedented humanitarian need with other important drivers being long-term climate change (Sengupta 2021; WFP and UNEP, 2018), conflict, and the economic crisis (OCHA 2023). Afghanistan has experienced several severe droughts in the past, including multiyear drought events (Chen et al., 2023; Tayfur and Alami 2022; Qutbudin et al., 2019; Alami et al., 2017; Dost et al., 2023; Bhattacharyya et al., 2004; Dost and Kasiviswanathan 2023). Qutbudin et al. (2019) used Global Precipitation Climatology Center (GPCC) gridded dataset based Standardized Precipitation and Evapotranspiration Index (SPEI) (Vicente-Serrano et al., 2010) to examine the changes in drought in Afghanistan during growing seasons for wheat, corn and rice and found increases in drought severity and frequency in Afghanistan over 1901–2010 period. More recently, Chen et al. (2023) reported similar findings but using station data based SPEI, to analyze droughts in Afghanistan during the last 40 years. Dost and Kasiviswanathan (2023) used monthly precipitation data from 23 stations to calculate and examine the trend in Standardized Precipitation Index (SPI) and found negative trends in the northwest regions of the country and positive trends increased in central and southeast regions. Collectively these studies highlight the peculiar long-term drought vulnerability of Afghanistan. This vulnerability has been emphasized by the recent sequential drought events over 2020 to 2023, that coincided with a multiyear La Niña event that started in July–September 2020 and

persisted until early 2023. The coincidence of multiyear La Niña with the sequential droughts highlights the importance of investigating the longer-term relationship between La Niña and droughts, and agricultural outcome in Afghanistan, with the overarching goal of supporting early warning of such events and their impacts in the future

ENSO influences the climate of Central Southwest Asia (which includes Afghanistan) via stationary Rossby waves forced by ENSO-related tropical convection (Alizadeh 2024; Alizadeh-Choozari 2017; Alizadeh-Choozari and Adibi, 2019; Barlow et al., 2002, 2021; Hoell et al. 2015a, 2015b, 2017, 2018, 2020; Huang and Stevenson 2023; Lenssen et al., 2020; Mariotti 2007; Phillips et al., 1998; Syed et al., 2006). For example, Mariotti (2007) finds ENSO’s influence on precipitation in this region to be strong throughout the rainy season, and highlights the role of a southwesterly (northeasterly) circulation pattern during El Niño (La Niña) that enhances (dampens) moisture input into this region (Hoell et al., 2012, 2015a). However, like in the case of Mariotti (2007), ENSO’s influence on Afghanistan’s climate has been primarily investigated in terms of its impacts on cold season precipitation, frequently at a seasonal scale (often November to April) and at a monthly scale in at least one study (Hoell et al., 2015b). These studies focused on changes in seasonal precipitation in the region at a broad scale (Central Asia or Southwest Asia), using coarse scale precipitation datasets with scarce in situ data inputs (Hoell et al., 2015b, 2017; McNally et al. 2022; Syed et al., 2006). To our knowledge, in only two past studies, the impact of ENSO on seasonal climate in the region was examined using hydrologic variables other than precipitation. For example, Hoell et al. (2015b) demonstrated how the composites of dry and wet winter seasons, based on seasonal precipitation, broadly translated into changes in snow water

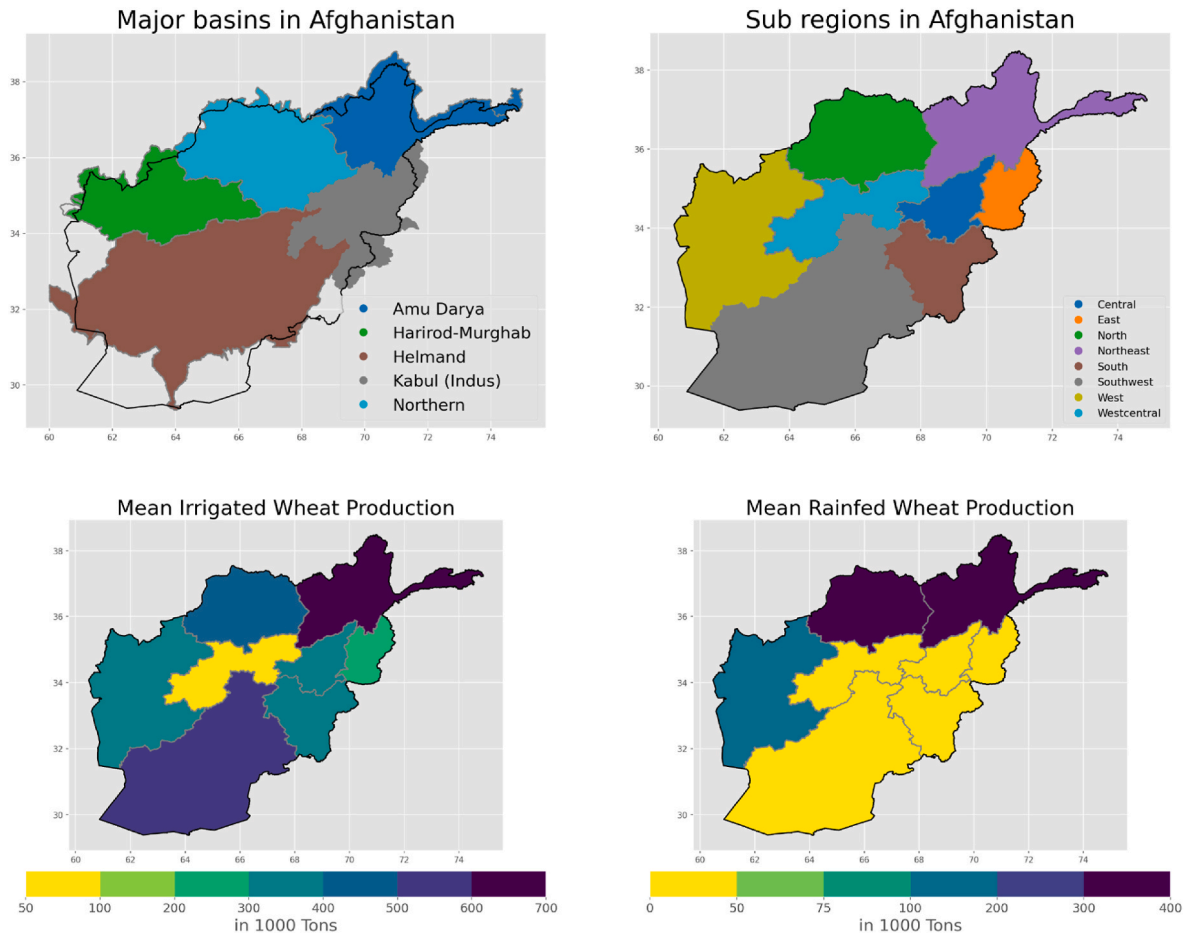


Fig. 1. Boundaries of the five of the major basins in Afghanistan (top left), boundaries of the sub-regions in Afghanistan (top right), mean irrigated wheat production aggregated over the sub-regions (bottom left), and mean rainfed wheat production aggregated over the sub-regions (bottom right)

equivalent, soil moisture, evapotranspiration and runoff in the region of southwest Asia. Hoell et al. (2020) examined the precursors and predictability of agricultural drought in the Amu Darya basin, using the Community Earth System Model simulations

Past research has undoubtedly established a clear link between ENSO and winter seasonal precipitation in Afghanistan, albeit as part of broader regional studies. However, we still lack the understanding of (a) the robustness (or lack thereof) of the relationship between ENSO events (La Niña versus El Niño) and snow drought, hydrological drought, and agricultural drought, and the extent to which both events impact irrigated and rainfed agricultural yield outlook and (b) the spatial variability in the probability of drought and severity of impacts. Understanding of ENSO's influence on snow is critical given its importance in Afghanistan's water supply (Muhammad et al., 2017), which is the main source of water for irrigated agriculture. By some estimates, 86% of the irrigation area is supported by rivers and springs (Rout 2008). Moreover, rainfed agriculture, a smaller contributor to overall agricultural production (Fig. 1), is still critical for local food availability and agricultural labor opportunities (Aliyar et al., 2022) and is largely dependent on the spring rains. Past studies have not specifically examined the impacts of ENSO on rainfed agriculture across the country, noting that rainfed agriculture, like irrigated agriculture, is distributed across the country. Which parts of rainfed and irrigated agriculture areas are most vulnerable to ENSO-related drought events is not clearly understood. The understanding of the influence of ENSO on drought in each of those areas is also critical to support any adaptation measures (Aliyar et al., 2022) during future ENSO events

Finally, the agro-climatological monitoring to support food insecurity early warning is done by agencies such as United States Agency for International Development's Famine Early Warning Systems Network (FEWS NET) (Funk et al. 2019) and the Group on Earth Observations Global Agricultural Monitoring Initiative (GEOGLAM) (Becker-Reshef et al. 2010; 2020). The monitoring is conducted by convergence of evidence, relying on several earth observation datasets (such as rainfall, soil moisture, normalized difference vegetation index (NDVI), and reservoir level) to understand the spatial variability in drought development and progression and its severity. The knowledge provided by past research on the variability of seasonal precipitation with ENSO events is not sufficient to meet the needs of the early warning agencies that tend to rely on several indicators (as listed above) in addition to precipitation

Therefore, we build upon past research on the effect of the ENSO on Southwest Asia and Central Asia, including Afghanistan (Alizadeh-Choozari 2017; Barlow et al., 2002, 2021; Hoell et al., 2015b, 2017, 2018, 2020; Mariotti 2007; Syed et al., 2006) and specifically seek to answer the central question: "What is the influence of ENSO on the drought outlook and agricultural outcome in Afghanistan and how does that influence vary spatially?" We conduct a comprehensive and detailed examination of the relationship between ENSO and drought outlooks in Afghanistan to address the existing critical gaps in our understanding. We do so by relying on several satellite and simulated datasets (Table 1) that provide a better understanding of the ENSO related diversity in the probability of meteorological, snow, hydrological, and agricultural droughts and the spatial variability in ENSO influence on agricultural outcomes, represented by agropastoral livelihood zones and wheat reports. This study's overarching goal is to advance the understanding of ENSO's influence on drought outlooks in Afghanistan to strengthen early warning of drought and associated acute food insecurity in Afghanistan, which as highlighted above, is one of the most food insecure regions globally. In the next sections, we provide a brief overview of the earth observational datasets used in this study (Table 1), the results of ENSO impact on drought analysis, and the implications of the results in improving early warning of drought impacts related to future ENSO events

2. Data

Table 1

Typology of droughts and agricultural outcome, and corresponding datasets, analyzed in this study.

Meteorological Drought	Standardized Precipitation Index (SPI) based on: (1) CHIRPS (https://data.chc.ucs.edu/products/CHIRPS-2.0/global_3-monthly_EWX/zscore/) (2) GPCC (https://psl.noaa.gov/data/gridded/data.gpcc.html) (3) APHRODITE (https://www.chikyuu.ac.jp/precip/english/products.html) (4) ERA5-Land Precipitation (https://cds.climate.copernicus.eu/cdsapp#!/dataset/reanalysis-era5-land-monthly-means?tab=form) (5) PERSIANN-CCS-CDR (https://chrsdata.eng.uci.edu/) Standardized Precipitation and Evapotranspiration Index (SPEI) based on: (1) CHIRPS (https://data.chc.ucs.edu/products/CHIRPS-2.0/global_monthly/netcdf/) (2) Hobbins reference evapotranspiration dataset (https://data.chc.ucs.edu/products/Hobbins_RefET/ETos_p05_dekad_global/tifs/) SPEI data for Afghanistan also available via https://data.chc.ucs.edu/people/husak/forShrad/
Snow Drought	Snow Water Equivalent from: (1) FEWS NET Land Data Assimilation System (FLDAS) (https://disc.gsfc.nasa.gov/datasets?keywords=FLDAS) (2) ERA5-Land (https://cds.climate.copernicus.eu/cdsapp#!/dataset/reanalysis-era5-land-monthly-means?tab=form)
Hydrological Drought	(1) Runoff data from FEWS NET Land Data Assimilation System (FLDAS) (https://disc.gsfc.nasa.gov/datasets?keywords=FLDAS) (2) Water level data (https://dahiti.dgfi.tum.de/en/3779/water-level-altimetry/)
Agricultural Drought	(1) Evaporative Stress Index (https://climateserv.servirglobal.net/) (2) NDVI (https://earlywarning.usgs.gov/fews/datado wnloads/EastAfrica/NDVIeMODIS)
Agricultural Yield Report	FEWS NET Data Explorer (https://fdw.fews.net/data-explorer/crop)

To investigate the relationship of ENSO events with the probability of drought and agricultural outcomes (measured by reported crop yield) in Afghanistan, this study relies on several datasets that cover varying record lengths, some extending to 1981 and some others to ~2000s. Table 1 lists the drought indicators, corresponding datasets and download links. We use the full record of all datasets to test the robustness of the ENSO relationship with the probability of drought and impacts on agricultural outcome throughout the time period

1.1. Standardized Precipitation index

We use the Standardized Precipitation Index (SPI) (McKee et al., 1993) to analyze the influence of ENSO events on meteorological droughts (Table 1). SPI is widely used to estimate drought severity, duration, and frequency based on precipitation data, and SPI has been previously used in past studies focused on analyzing drought conditions in Afghanistan (Alami et al., 2017; Dost et al., 2023; Tayfur and Alami 2022). The SPI transforms the precipitation record into a standardized value that represents the number of standard deviations by which the observed precipitation value deviates from the mean. Positive values of SPI indicate wetter than average conditions, while negative values indicate drier than average conditions. SPI values below -0.44 are considered to be in the lower tercile with an associated climatological probability of occurrence of 33%. In this analysis, we calculate SPI-3 (i.e., SPI calculated over a 3-month season, hereafter referred as SPI) for October to December, December to February, and March to May seasons, which mark seasons important for planting decisions for winter wheat, snow accumulation for irrigated wheat, and rainfed farming of spring wheat, respectively. SPI was calculated over 1981–2022 following the methods described in (Husak et al., 2007) at 0.05-degree

spatial resolution using the Climate Hazards Infrared Precipitation with Stations (CHIRPS) dataset (Funk et al. 2015a, Funk et al., 2015b). CHIRPS is a quasi-global rainfall dataset that combines satellite-derived, infrared, temperature-based precipitation estimates with in situ station data. CHIRPS is a widely used dataset that has been previously used in studies focusing on central southwest Asia and Afghanistan (McNally et al. 2022; Nabizada et al., 2022)

1.2. Standardized Precipitation Evapotranspiration Index

In addition to SPI, we also examined the influence of ENSO on climatic water balance and associated drought, using the Standardized Precipitation Evapotranspiration Index (SPEI) dataset (Vicente-Serrano et al., 2010) (Table 1). The SPEI has been used for analyzing drought characteristics and its spatiotemporal variability in Afghanistan in multiple past studies (Chen et al., 2023; Qutbudin et al., 2019). The method of calculation of SPEI is largely similar to SPI but it is based on the difference between precipitation and potential evapotranspiration. We follow the method described in Vicente-Serrano et al. (2010) to calculate SPEI. CHIRPS was used as the precipitation dataset, along with potential evapotranspiration (Hobbins et al., 2016) derived using MERRA-2 based atmospheric forcings (Gelaro and Coauthors, 2017). Hobbins et al. (2023) describes in detail the methodology of generating potential evapotranspiration using the MERRA-2 atmospheric forcings. The spatial resolution of SPEI data is 0.05°, and the dataset goes back to 1981. We examined SPEI during the October–December to March–May seasons covering the critical parts of the growing seasons for both irrigated and rainfed agriculture

The application of SPEI for this study allows for the examination of any temperature related impacts on the climate water balance beyond precipitation related impacts depicted by SPI. Given the temperature trends in Afghanistan, its influence on the climate water balance as indicated by long-term changes in SPEI was also highlighted in the World Food Programme (WFP) and United Nations Environmental Programme (UNEP) report examining the influence of climate change in food security in Afghanistan (WFP and UNEP, 2018). SPEI is also routinely used as an indicator of agriculture drought outcome by the FEWS NET in Afghanistan (personal communication with FEWS NET's regional scientists who focus on Afghanistan, 2023; 2024)

1.3. FEWS NET Land Data Assimilation System based hydrologic simulations

In addition to meteorological drought indicators for snow dominated regions in Afghanistan using indicators that account for snow accumulation and melt is important (Muhammad et al., 2017). However, given the lack of in situ reports of snow and snowmelt driven runoff, we use FEWS NET Land Data Assimilation System (FLDAS) (McNally et al. 2017) simulated hydrologic variables to analyze the relationship between ENSO on snow and hydrologic drought (Table 1). The FLDAS simulated snow and runoff products are routinely used for monitoring drought conditions in Afghanistan (Becker-Reshef et al. 2020; McNally et al. 2022). The FLDAS simulations used in this study are driven by the CHIRPS precipitation dataset (Funk et al., 2015a) and temperature, wind, and radiation forcings from MERRA-2 (Gelaro and Coauthors, 2017) reanalysis (which is also used to generate potential evapotranspiration (PET) dataset for SPEI calculation, section 2.2). The simulation is at a gridded spatial resolution of 0.1° (or ~10 km), available in near real-time (about 3 weeks after the end of the month) and extends to 1981, making it an important dataset for hydrologic monitoring in Afghanistan (McNally et al. 2022). The simulations are available at a daily scale, but for this analysis we aggregated them to calculate mean seasonal snow water equivalent (SWE) over the January to March season, as an indicator of snow drought, and total water year (WY) seasonal runoff (sum of daily surface and subsurface runoff simulation over October to September), as an indicator of hydrologic drought. We then

convert the seasonal values to standardized anomalies and examine the probability of achieving below normal (<-0.44) values during La Niña versus El Niño years. Additionally, to highlight the changes in basin aggregated absolute values of seasonal SWE (total WY runoff) we calculated the volume of both quantities by multiplying the mean depth values by the grid cell area, and then we calculated the average (sum) across major basins in Afghanistan (Fig. 1)

1.4. Evaporative stress index

We also use remotely sensed Evaporative Stress Index (ESI) (Anderson et al., 2011) (Table 1), which is typically considered as an indicator of agricultural drought, as an independent dataset to examine the influence of ENSO on moisture available for crop growth. The ESI has been used previously used for agricultural drought monitoring in South Asian countries including Afghanistan and described as a superior indicator of drought with greater sensitivity, relative to other vegetation condition indicators such as vegetation health index (VHI), enhanced vegetation index (EVI), and standardized anomaly index (SAI) (Shahzaman and Coauthors, 2021). The ESI spans back to the 2000s and is widely used for monitoring and early warning of rapidly developing “flash drought” events (Otkin et al., 2018) and agricultural droughts (Yang and Coauthors, 2018). The ESI is based on remotely sensed land surface temperature (LST). The LST measurements are used to estimate water loss due to evapotranspiration and are then compared to the evapotranspiration (ET) in the case of an adequate supply of water. Healthy vegetation with adequate levels of ET warms at a much slower rate than vegetation experiencing a lack of water supply resulting in reduced ET. Hence, based on variations in LST at a given time relative to its average value the ESI indicates how the current rate of ET compares to normal. Negative ESI values indicate vegetation that is moisture stressed and vice versa. This product is available at 5-km spatial resolution and at near real-time (Table 1). Two versions of ESI products vary in the cumulative duration over which they track the moisture stress. We use the ESI-12 week product that monitors the ET stress over 12 weeks, about a 3-month season. The application of ESI in this analysis increases the number of independent datasets because SPI, SPEI, and FLDAS all rely on CHIRPS precipitation and makes this result directly relevant for early warning agencies that use ESI for drought monitoring (such as GEOGLAM's Crop Monitor for Early Warning). The ESI data were downloaded from SERVIR's ClimateSERV (<https://climateserv.servirglobal.net/>)

1.5. Reservoir water level data

We use satellite altimetry based estimates of the water level at the Kajaki reservoir provided by the Database for Hydrological Time Series of Inland Waters (DAHITI) project (Schwatke et al., 2015) (Table 1). The Kajaki reservoir is one of the two main reservoirs in heavily irrigated Helmand province (Goes et al., 2016) in southern Afghanistan. The long-term record (going back to 1991) of water level only exists for the Kajaki reservoir, with the data for other reservoirs in Afghanistan being limited to generally 2016 and in a few cases to 2008. The water level data is based on inland water body monitoring from satellite altimetry by application outlier rejection and a Kalman filter approach on ensemble of cross-calibrated altimeter data from several sources such as Envisat, ERS-2, Jason-1, Jason-2, TOPEX/Poseidon, and SARAL/AltiKa, including their uncertainties (Schwatke et al., 2015). It is important to note that reservoir water level can be affected by non-climatic management decisions, nonetheless this dataset is routinely used for monitoring water availability in Afghanistan by FEWS NET. The water level data were manually downloaded using this link: <https://dahiti.dgfi.tum.de/en/3779/water-level-altimetry/>

1.6. Normalized difference vegetation index

We use the Normalized Difference Vegetation Index (NDVI) which is an indicator of vegetation health and productivity to examine the influence of ENSO on agricultural drought (Table 1). The NDVI is a commonly used metric for vegetation health, and is calculated by comparing the reflectance of near-infrared and visible red light. Healthy vegetation absorbs more near-infrared light and reflects more visible red light, resulting in a higher NDVI value. The spatial resolution of this dataset is 250 m. For this analysis, we use the Expedited Moderate Resolution Imaging Spectroradiometer (eMODIS) NDVI (Jenkerson et al., 2010), which goes back to 2002. Until recently, MODIS NDVI was a widely used product for agricultural drought and crop yield/production monitoring (Brown and de Beurs 2008; Funk and Budde 2009; Groten 1993; Shukla et al., 2021) and forecasting (Lee and Coauthors, 2022) to monitor vegetation conditions in Afghanistan and beyond. Since late 2022 this product has been replaced by Visible Infrared Imager Radiometer Suite (VIIRS) NDVI (Skakun et al., 2018), but, at the time of this analysis, that dataset only goes back to 2012 making it unsuitable for this analysis, so we relied on eMODIS NDVI (hereafter referred to as NDVI). The NDVI values are available on a dekadal basis, which we convert to monthly by taking the mean of the dekadal NDVI values. We then convert the monthly values of NDVI to standardized anomalies using the climatology over 2003 to 2022. The eMODIS NDVI data were downloaded from the U.S. Geological Survey (USGS) FEWS NET Data Portal (<https://earlywarning.usgs.gov/fews>).

1.7. Wheat reports

Finally, we also use available reports of irrigated and rainfed wheat production and harvest area over the 2002–2022 period (Table 1). The data for the 2002–2019 period are available at province level (Fig. S4) and is sourced from the Afghanistan Ministry of Agriculture, Irrigation and Livestock (MAIL). The data for 2012 to 2023 is sourced from the United States Department of Agriculture's Foreign Agricultural Service's Production Supply and Distribution (USDA PSD). This dataset is only available at national scale and for total (irrigated + rainfed) wheat production and harvested area. We performed some basic quality controls on the MAIL data, correcting for typos and miscalculations. We also converted the MAIL data to sub-regional yield data (Fig. S4) by summing the production values of all the provinces within a given sub-region (as shown in Fig. 1) and dividing by the total sum of the harvested area of those provinces. The primary reason for aggregating the yield data from province to sub-regional level was to attempt to reduce the influence of uncertainties in the data at province scale. Fig. 1 shows the mean irrigated and rainfed wheat production in each of the sub-regions during the 2002–2019 period based on the data from MAIL.

As can be seen in Fig. S4, the sub-regional yield values are lower in the initial part of the record versus later part of the record. To account for this non-stationarity in the yield data we detrend the data by converting yield data into anomalies based on the 5-year moving average centered on the target year. For the first two and the last two years of the record (which would not have a sufficient record in a 5-year window centered on those years) we use the closest 5 years including the target year to calculate the 5-year moving average.

2. Methods

This section describes the methods used for identifying ENSO events, for calculating probability of below normal events, and for statistical significance testing.

2.1. El Niño-southern oscillation events

In this study, we follow Climate Prediction Center's (CPC) classification of ENSO events which is based on the Oceanic Niño Index (ONI

(Huang and Coauthors, 2017). Per this classification, since 1981, a total 13 El Niño events and 15 La Niña events are included in this analysis. El Niño events include 1982/1983, 1986/1987, 1987/1988, 1991/1992, 1994/1995, 1997/1998, 2002/2003, 2004/2005, 2006/2007, 2009/2010, 2014/2015, 2015/2016, 2018/2019, and La Niña events include 1983/1984, 1984/1985, 1988/1989, 1995/1996, 1998/1999, 1999/2000, 2000/2001, 2005/2006, 2007/2008, 2008/2009, 2010/2011, 2011/2012, 2017/2018, 2020/2021, 2021/2022. In the case of NDVI, ESI, and wheat reports, which go back to 2002/2003, El Niño and La Niña events are reduced to 7 and 8 events, respectively.

2.2. Probability of below normal and statistical significance testing

We converted each of the drought indicators into standardized anomalies as described in section 2 using each of the datasets' full climatology. We then counted the number of times standardized anomalies for any given indicator, season, and pixel were below -0.44 , which is the threshold of the lower tercile category, and divided that by the total number of events equivalent to the length of the record (e.g., 42 years for the datasets spanning over 1981–2022). Subsequently, we calculated the statistical significance of the probability of below normal events following the method used by Mason and Goddard (2001). The null hypothesis (H_0) is that the occurrence of below-normal events is solely attributable to random chance, considering the total number of observed events and the number of El Niño or La Niña events and the alternative hypothesis (H_a) is that the observed frequency of below-normal events is significantly different from what would be expected by chance alone. Finally, for the El Niño or La Niña composites of wheat yield, we conducted a Wilcoxon Rank Sum Test (Wilks 2011) given the null hypothesis that both of those composites belong to the same population.

3. Results

Here we present the results of our analysis investigating the influence of ENSO on the probability of drought outlook and agricultural outcome. Given the lack of (often nonexistent) observed record of water availability and agriculture statistics, we rely on several datasets ranging from modeled to remote sensing based datasets. Rather than focusing on any linear relationship between ENSO and the above-mentioned indicators, we focus on examining how the likelihood of drought, in this case, defined by a below normal tercile event, changes during the La Niña events relative to El Niño events. Our focus on this question is due to its important implications for food insecurity early warning in Afghanistan.

3.1. ENSO based meteorological drought outlook

We start the examination of ENSO influence on meteorological drought by focusing on the probability of the SPI being in the lower tercile during early-winter (October–December), mid-winter (December–February), and spring (March–May) season in La Niña versus El Niño years (Fig. 2). The chances of receiving below normal SPI greatly increases during La Niña years versus El Niño years. In general, over much of the country, during early-winter, the probability of SPI being below normal is $>50\%$ during La Niña years, with the main exception being parts of the Southwest region. The probability is statistically significant mainly in parts of West, North, and Northeast regions. When focusing on mid-winter precipitation, the highest probability (reaching above 80% in some cases) with statistical significance, is seen in North, West, and West Central regions during La Niña years. In the case of spring season, which is critical for rainfed agriculture, the statistical significance of the probability of below normal during La Niña, is limited to parts of the West.

Finally, the probability of meteorological drought during El Niño events is generally below climatological probability (33%) almost across

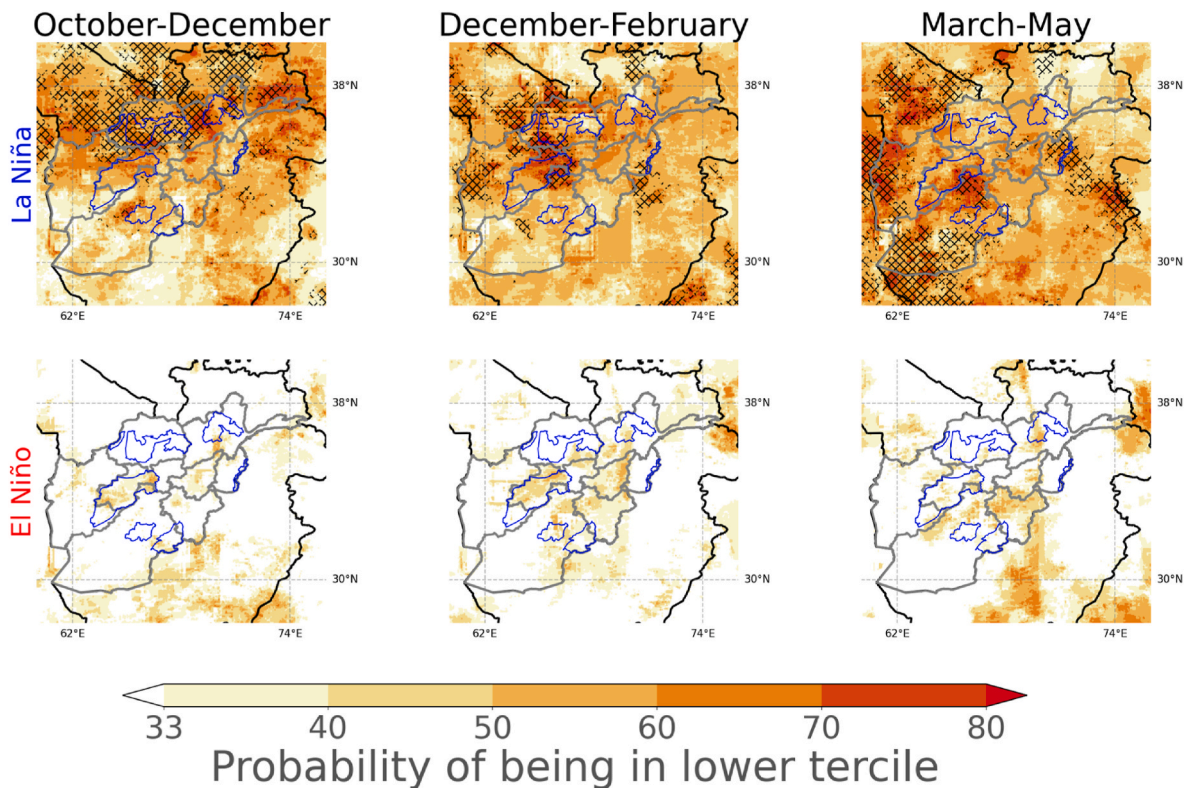


Fig. 2. Probability of Standardized Precipitation Index (SPI) being in the lower tercile in October–December, December–February and March–May seasons. The blue color polygons indicate Famine Early Warning Systems Network (FEWSNET) livelihood zones that rely on rainfed agriculture, and the gray color polygons indicate the boundary of the main sub-regions in Afghanistan (as in Fig. 1). Statistical significance at 95% confidence level is indicated by the hatches (For interpretation of the references to color in this figure legend, the reader is referred to the Web version of this article.)

the country (Fig. 2). For early warning purposes, this is a key piece of information, as at least climatologically this indicates a clear increase in the chances of meteorological drought development during La Niña versus El Niño years

We also examine the probability of meteorological drought as per SPEI (Fig. 3). In general, we find similar patterns in the increased probability of drought in the North, West, and Northeast regions, as we did using SPI. Similar to those results, the probability of drought during El Niño years is also generally less than the climatological probability. The one notable difference between the SPI and SPEI based probability of drought is the statistical significance of the probability of spring season SPEI drought being over a much larger region of the North and the West sub-regions. As shown in Fig. 1, the North and West sub-regions are among the main rainfed wheat producers in the country. The statistical significance of SPEI drought (versus SPI drought) may be due to La Niña's influence on evaporative demand in this season beyond its influence on precipitation alone

3.2. ENSO based snow drought outlook

Fig. 4 shows the probability of snow drought during La Niña versus El Niño years during January–March (JFM) which generally marks the peak of the snow accumulation period (Fig. S1). The probability of SWE being below normal is generally higher than 50% across the region with the highest probability in parts of the Amu Darya basin and nearby regions. The probability of below normal JFM SWE is also statistically significant in the northern parts of the Amu Darya basin

To further understand the impact of La Niña on SWE, in Fig. 5 we show the range of SWE volume (in cubic meters) for each of the five major basins, during La Niña versus El Niño years, since 1981. Across the basins, in general, SWE during JFM seasons has been lower during the La Niña years versus El Niño years. Although as the composites indicate

there have been exceptions to this general pattern

To better appreciate the extent of the impact of La Niña on SWE we also calculated the difference in the median of the SWE volume composites during La Niña versus El Niño years (Fig. 5). Here, the basins are ordered based on the proportion of the Afghanistan water supply attributed to a given basin, with the Amu Darya [Northern] basin being the highest [lowest] contributor to water supply as per Rout (2008). This analysis indicates that on average La Niña has resulted in about 30% reduction in SWE volume in the Amu Darya basin with the estimates for other basins ranging from 9 to 35% reduction. In the absence of long-term snow observations, this modeled estimate at least provides a sense of the magnitude of the loss in SWE attributable to La Niña years

Finally, Fig. 5 also shows the upper and lower tercile of the SWE (over 1981–2022) for each of the basins. In general, the median SWE during La Niña events tends to be closer to the lower tercile, and the median SWE during El Niño events tends to be closer to the upper tercile values

3.3. ENSO based hydrologic drought outlook

The impact of La Niña related rainfall and snow drought on hydrologic drought are further highlighted in Figs. 6–8. This analysis relies on the gridded modeled estimates of total runoff (sum of surface and sub-surface runoff) (Figs. 6 and 7) and observational estimates of water level in one of the major reservoirs in Afghanistan (Fig. 8), as indicators of hydrologic drought. Fig. 6 shows the probability of March–July (MAMJJ) runoff being below normal during La Niña versus El Niño years. In general, runoff tends to be higher during those months as shown in Fig. S1

The probability of below normal MAMJJ runoff is considerably higher during La Niña years, often above 50%, with the main exceptions being the part of the Southwest region in the Helmand basin (Fig. 6). The

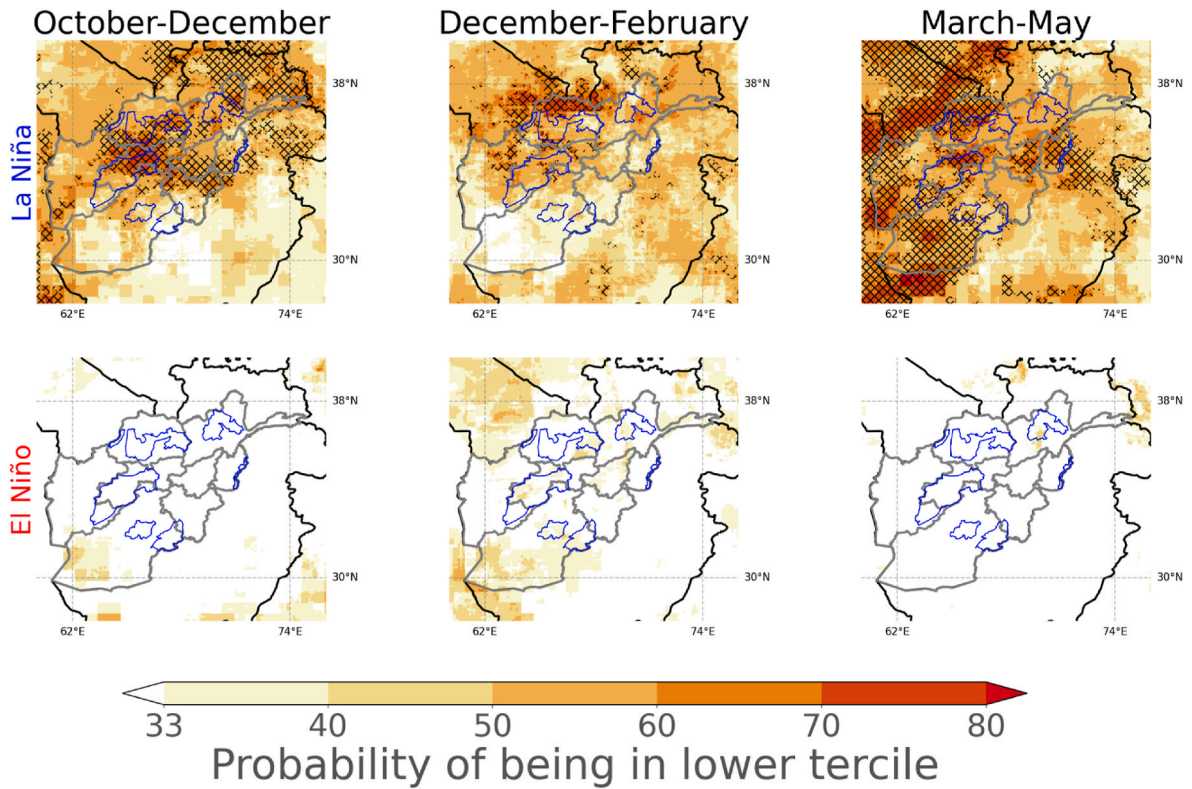


Fig. 3. Probability of Standardized Precipitation Evapotranspiration Index (SPEI) being in lower tercile in October–December, December–February and March–May seasons. The blue color polygons indicate Famine Early Warning Systems Network (FEWS NET) livelihood zones that rely on rainfed agriculture, and the gray color polygons indicate the boundary of the main sub-regions in Afghanistan (as in Fig. 1). Statistical significance at 95% confidence level is indicated by the hatches (For interpretation of the references to color in this figure legend, the reader is referred to the Web version of this article.)

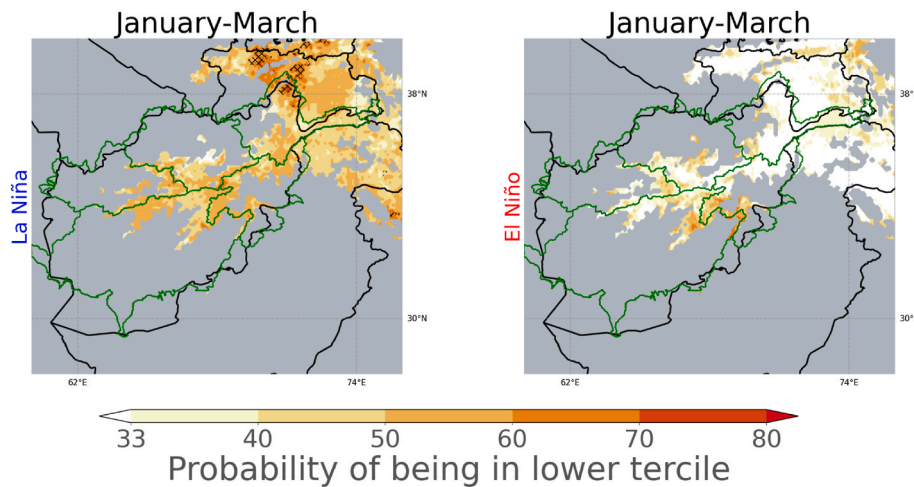


Fig. 4. Probability of standardized snow water equivalent (SWE) anomalies being in lower tercile in January–March season, which is the peak of the snow accumulation season in Afghanistan. The green color polygons indicate the boundaries of five of the major basins in the country. The probability values are only shown for grid cells that climatologically receive at least 10 mm of SWE during the month of March. Statistical significance at 95% confidence level is indicated by the hatches (For interpretation of the references to color in this figure legend, the reader is referred to the Web version of this article.)

probability of below normal runoff is the highest in the Northern basin, western Hariord-Murghab basin, western parts of Helmand basin, and parts of Kabul basin. All those basins include sub-regions with irrigated wheat production (Fig. 1). The probability of drought during El Niño years is generally below 33% across the country

Again, in order to provide a better understanding of the impact of La Niña on hydrologic drought (and water availability), in Fig. 7 we show the composites of runoff volume aggregated over the MAMJJ season in

respective basins, for La Niña versus El Niño years. We also calculate the percentage difference in the median values of both composites to provide modeled estimates of decrease in water supply during La Niña years relative to El Niño years. These estimates of reduction in MAMJJ total runoff vary from 28% to 42%. In this figure as well, the order of basins is according to their contribution to the water resources of Afghanistan. In the top three contributing basins, the reduction in total runoff volume ranges from 28% to 34%. This reduction in total runoff is likely to mean

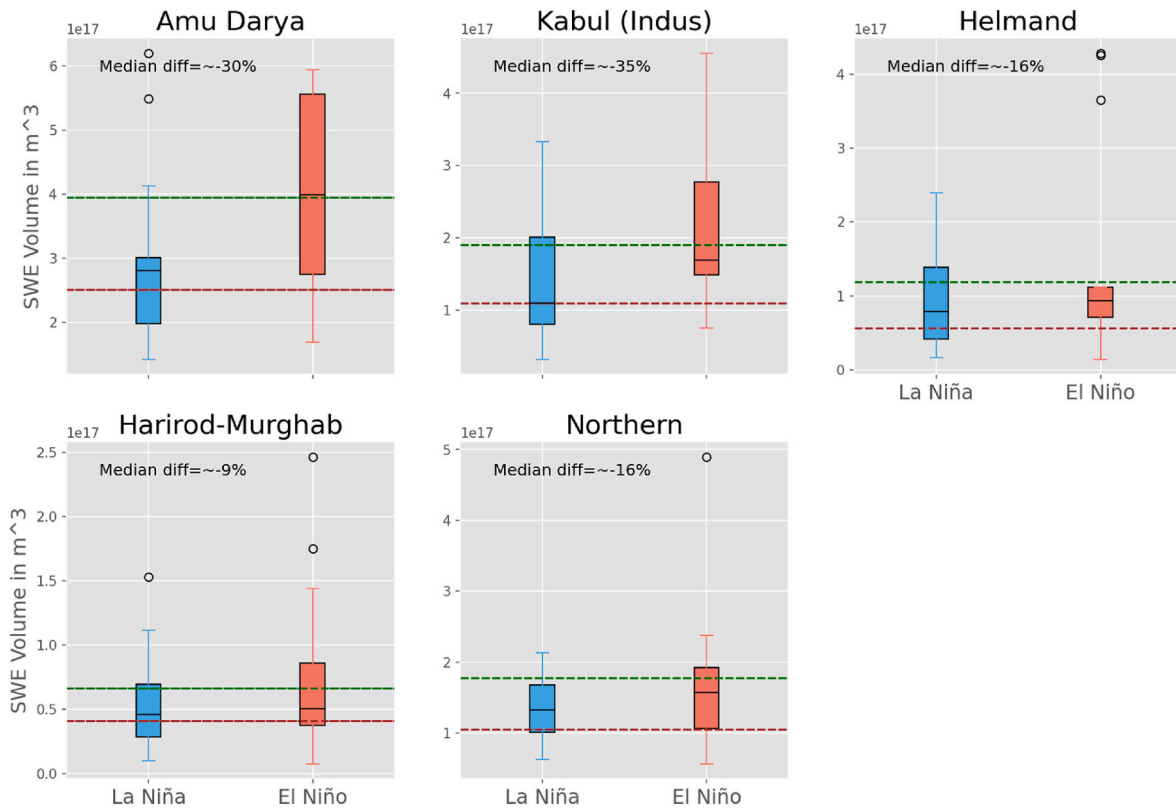


Fig. 5. Composites of basin-accumulated snow water equivalent (SWE) volume during La Niña (blue box) and El Niño (red box) years in five of the major basins in the country. The black line inside the box shows the median of SWE composites. The corresponding whisker caps display the values within 1.5 times the interquartile range at both ends. The circle markers show the outliers beyond that range. Differences in the median (i.e. Median diff) of each composite for each of the basins are also shown. The green [brown] dotted line indicates the upper [lower] tercile. Number of El Niño [La Niña] events is 13 [15] respectively. (For interpretation of the references to color in this figure legend, the reader is referred to the Web version of this article.)

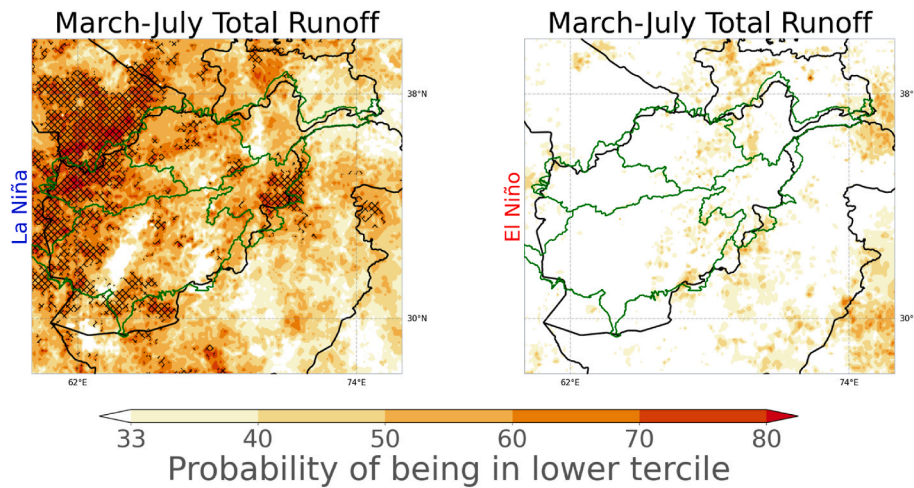


Fig. 6. Probability of standardized total water year runoff anomalies being in lower tercile. The green color polygons indicate the boundary of five of the major basins in Afghanistan. Statistical significance at 95% confidence level is indicated by the hatches. (For interpretation of the references to color in this figure legend, the reader is referred to the Web version of this article.)

decreased water availability for irrigation during the La Niña years in those regions

Next, we also examine the ENSO impacts on the reservoir level in Afghanistan. The water level generally is the lowest during the start of the water year, attaining its peak in May. We compare the composites of standardized anomaly of the mean WY water level during La Niña and El Niño years (Fig. 8, top left panel). During La Niña years the standardized anomalies are generally lower than El Niño years. The median

standardized anomaly during La Niña [El Niño] years being ~ -0.6 [$\sim +0.8$]. We also show the standardized anomalies for individual years in the same figure (top right panel), which helps highlight (a) the general pattern of WY water level anomalies being below 0 during La Niña years and above 0 being in the El Niño years, and (b) the exceptions to that general pattern, and (c) the lowest water levels on record coincided with double La Niña years (2 consecutive La Niña years)

We also display (Fig. 8, bottom panel) the absolute water levels in

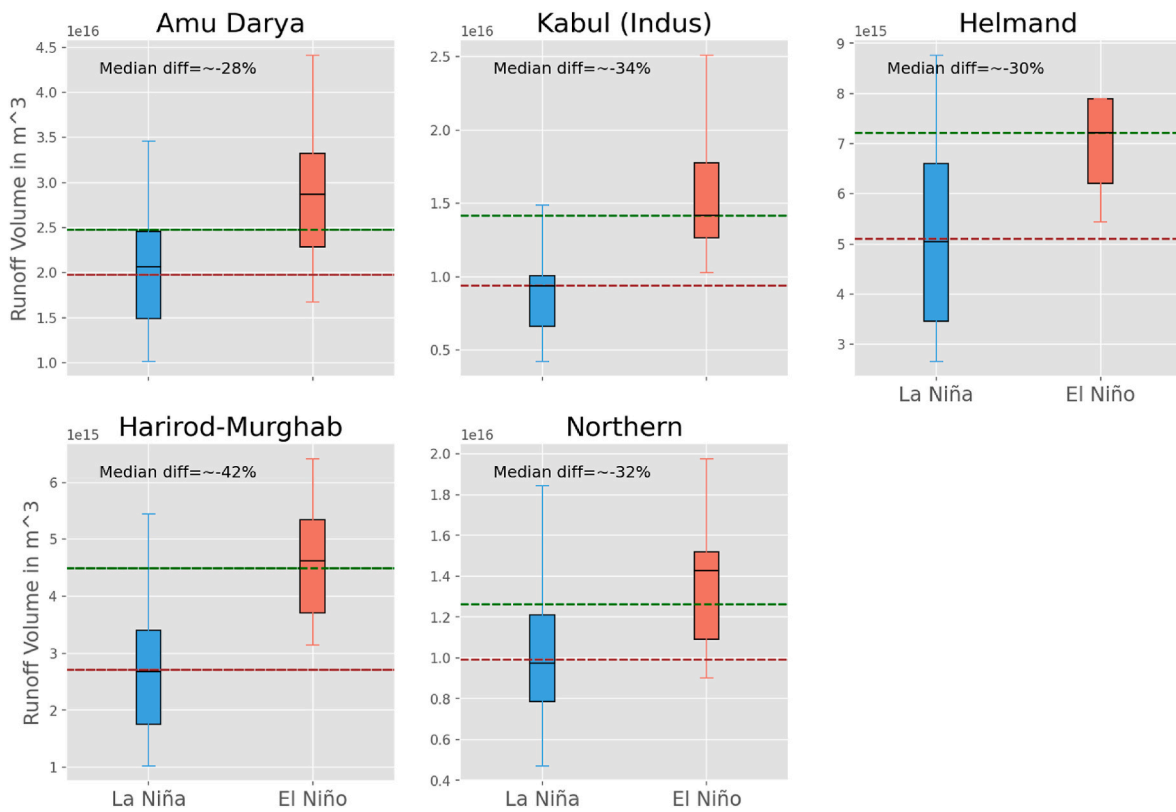


Fig. 7. Composites of basin accumulated March–July total runoff volume during La Niña and El Niño years in five of the major basins in Afghanistan. The black line inside the box shows the median of runoff composites. The corresponding whisker caps display the values within 1.5 times the interquartile range at both ends. The circle markers show the outliers beyond that range. Differences in the median (i.e. Median diff) of each composite for each of the basins are also shown. The green [brown] dotted line indicates the upper [lower] tertile. Number of El Niño [La Niña] events is 13 [15], respectively (For interpretation of the references to color in this figure legend, the reader is referred to the Web version of this article.)

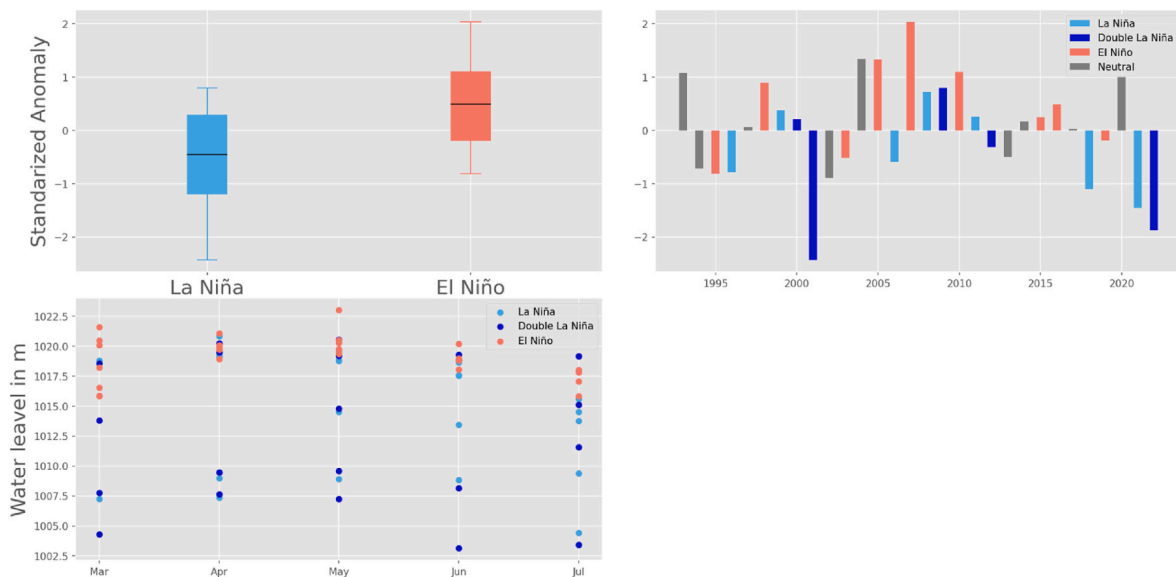


Fig. 8. Composites of standardized anomalies of mean water year (WY) water level during La Niña and El Niño years in Kajaki reservoir (Top left). The black line inside the box shows the median of each composite. The corresponding whisker caps display the values within 1.5 times the interquartile range at both ends. Standardized anomalies of mean WY water level for each of the years between 1991 and 2022, with the color of each bar indicating if the year was La Niña, Double La Niña, El Niño, or Neutral year (Top right). Monthly water level for March–July month when the water level is generally the highest in a given WY for each of the years where color of the solid dots shows if the year was La Niña, Double La Niña, or El Niño (Bottom Left) (For interpretation of the references to color in this figure legend, the reader is referred to the Web version of this article.)

Kajaki reservoir during the MAMJJ months of La Niña, double La Niña and El Niño years. Here we focus on MAMJJ months as typically the water levels tend to be the highest during that period of the year. The distinction in water level during La Niña and El Niño years during individual months' water level is apparent here as well. Water level tends to be lower during La Niña years than during El Niño years. Water level reached below 1 015 m during La Niña years only with the lowest values (up to ~1002 m) coinciding with double La Niña years. Conversely, the highest values, in general, coincided with El Niño years (with exceptions)

3.4. ENSO based agricultural drought outlook

Next, we focus on the impacts of ENSO on agricultural drought outlook using two widely used remote sensing based datasets, the Evaporative Stress Index (ESI) (Fig. 9) and eMODIS NDVI (Fig. 10). Fig. 9 shows the probability of ESI-12 being below normal from February to May, months that are crucial for both irrigated and rainfed wheat growing seasons. Note that ESI-12 for February [May] month depicts the average drought conditions over December to February [March to May] and so on

In general, the pattern of the regions with highest probability of agricultural drought (defined by $ESI < -0.44$) is consistent with what we have seen based on the preceding results. Agricultural drought during La Niña, as per ESI, is most likely to be experienced in North, West, and Northeast regions than in the rest of the country. The probability of drought seems to be higher during the 12 weeks ending in February and March than during the 12 weeks ending in April and May months. In North and Northeast regions, at least through April, the probability of below normal ESI is statistically significant, which would have important implications for agricultural production as those are among the main wheat producing regions in Afghanistan. Finally, consistent with previous results, the probability of agricultural drought, as per ESI, during El Niño years is almost always below 33%

We next examine the impacts of ENSO on agricultural drought outlook using eMODIS NDVI (Fig. 10). In this analysis, we also attempt to classify the influence of ENSO on agricultural droughts in rainfed versus irrigated regions (Pervez et al., 2014). We make use of the standardized anomalies of April NDVI values (similar results for May and

June NDVI are shown in Figs. S2 and S3), as in general, that is when the NDVI values start to peak in the country. Additionally, FEWS NET typically uses April NDVI values to provide first estimates of wheat production in the country, hence examination of April NDVI has a direct application of food insecurity early warning. Fig. 10 shows the probability of April NDVI being below normal during La Niña versus El Niño years in the rainfed regions (top panel) and irrigated regions (bottom panel). The mask used for classifying rainfed versus irrigated regions is based on eMODIS NDVI and was from Shahrari Pervez et al., 2014

The probability of below normal NDVI is particularly high in the rainfed regions, generally always above 60% and often above 80%, especially in the North, Northeast, and West sub-regions. The probability during El Niño years is generally below 33%, which is consistent with the analysis of different datasets thus far

The bottom panel shows the probability of below normal NDVI, but for irrigated regions, which has substantially higher implications for the food security in the country. This indicates that even in the irrigated parts of North, Northeast and West regions NDVI is likely to be below normal during the La Niña years. The probability of below normal for those regions is generally higher than 60%. This result indicates that both the irrigated and rainfed areas in this region experience adverse impacts due to La Niña, particularly in the North, Northeast, and West sub-regions of Afghanistan. In the rest of the irrigated regions, the estimates of the probability of April NDVI being below normal, are a little more mixed. The most notable is the NDVI over the intensively irrigated regions in southwest Afghanistan (in Helmand valley) where the probability values are closer to 33–40%

3.5. ENSO based agricultural yield outlook

Next, we examine ENSO based outlook of the agricultural yield. Fig. 11 shows the total wheat yield record time-series (top left) constructed using MAIL and USDA PSD data. We first compared the composites of total wheat yield at country level (note that USDA PSD data are only available at country level) for La Niña versus El Niño years. Although the median yield of El Niño composite is higher than that of La Niña, the difference between both composites is not statistically significant as per Wilcoxon Rank Sum Test

We then examine the effect of ENSO on wheat yield at sub-regional

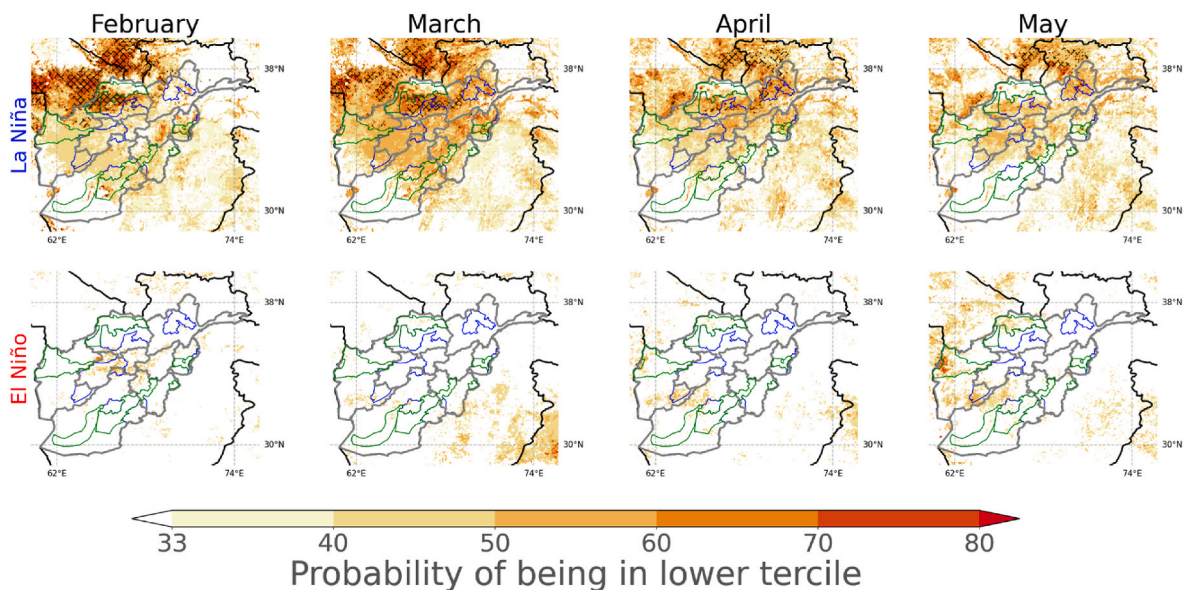


Fig. 9. Probability of evaporative stress index (ESI) during 12 weeks ending in the months of February through May, which are critical months during the wheat growing season. The blue color polygons indicate the boundary of the livelihood zone depending on the rainfed agriculture and the green polygons indicating the boundary of the livelihood zone depended on intensive irrigated agriculture. Statistical significance at 95% confidence level is indicated by the hatches (For interpretation of the references to color in this figure legend, the reader is referred to the Web version of this article.)

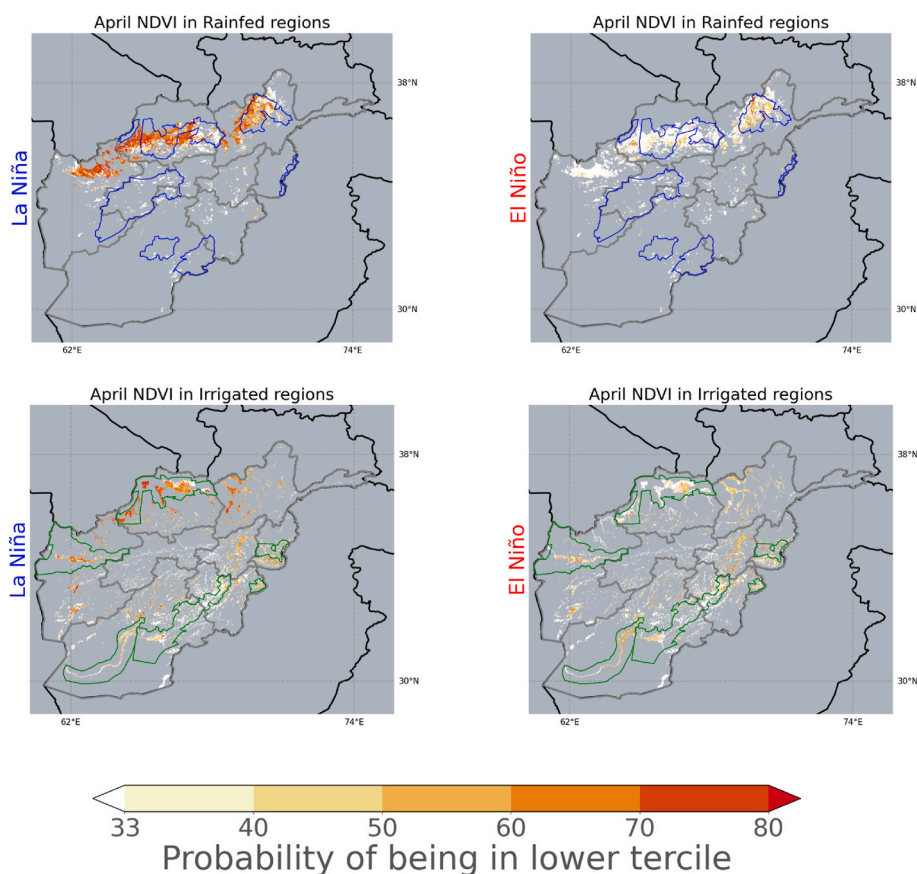


Fig. 10. Probability of standardized anomalies of mean April normalized difference vegetation index (NDVI) being in lower tercile during La Niña and El Niño years. The top figures show the probabilities in rainfed regions only and the bottom figures show the same for irrigated regions only. The blue color polygons indicate the boundary of the livelihood zone depending on the rainfed agriculture, and the green polygons indicate the boundary of the livelihood zone depending on intensive irrigated agriculture (For interpretation of the references to color in this figure legend, the reader is referred to the Web version of this article.)

scale for both irrigated (Fig. 11 bottom left panel) and rainfed wheat (Fig. 11 bottom right panel). The order of sub-regions is based on the order of the mean production for irrigated or rainfed wheat respectively. For irrigated wheat, we find a few instances when yield composite for La Niña years is lower than El Niño years, particularly in Southwest, North, and West regions (all of which are important producers of irrigated wheat) in the region but the difference in the composites is not statistically significant.

Whereas in the case of rainfed wheat yield we find more instances of La Niña composites being lower than El Niño years and at least a few cases when the difference between these composites is statistically significant at least at 90% confidence level. Those regions include Northeast, West, and South (significant at 90% confidence level) and Central region significant at 95% confidence level. It is important to note that the lack of statistical significance can also be due to data quality of wheat reports. Nonetheless, some of the important wheat producing regions do tend to have lower yields during the La Niña years than El Niño years, those regions include North, Northeast (mainly for rainfed), and West.

3.6. ENSO impacts as per historical food security and crop conditions reports

Lastly, we also examined the historical food security outlook reports produced by FEWS NET and GEOGLAM's CM4EW crop condition reports (<https://www.cropmonitor.org/crop-monitor-for-early-warning>) to verify the results of this study with documented impacts of past La Niña events on drought, agricultural production, and food insecurity in Afghanistan. The FEWS NET has been providing food security analysis in

Afghanistan since 2004, and CM4EW has been providing crop conditions reports over Afghanistan consistently since the 2016/2017 season.

In the FEWS NET's archive of food security outlook reports (<https://fews.net/middle-east-and-asia/afghanistan>), 2005/06, 2007/08, 2008/09, 2010/11, 2011/12, 2017/18, 2020/2021 and 2021/22 were La Niña years. Upon review of the food security outlook report that often comes out post June, coinciding with the harvest season, we find that in all the La Niña years, except for 2008/09 and 2011/12 seasons, agricultural production was adversely affected which contributed to a worsening of food insecurity outlooks. The FEWS NET reports frequently documented adverse impacts on North, Northeast, West rainfed areas and at least in a few cases, irrigated areas in that region as well, consistent with the findings of this study (Table 2).

Additionally, in the short archive (going back to 2016/2017 only) of CM4EW crop conditions reports for Afghanistan "Winter Wheat" (mainly irrigated) and "Spring Wheat" (mainly rainfed) season also indicated "Failure" and "Poor" conditions for "Spring Wheat" during the harvest following the 2017/18 and 2020/2021 La Niña events, particularly in the northern and northeastern regions (<https://www.cropmonitor.org/archive>). In both cases, the "Winter Wheat" conditions (mostly irrigated) in North and Northeast regions were also indicated to be "Poor" or "Failure" (Fig. 12).

Thus, the FEWS NET food security outlook report archive and CM4EW reports archive are also generally consistent with the findings based on multiple drought indicators used in the analysis, regarding the adverse impacts of La Niña on drought in Afghanistan.

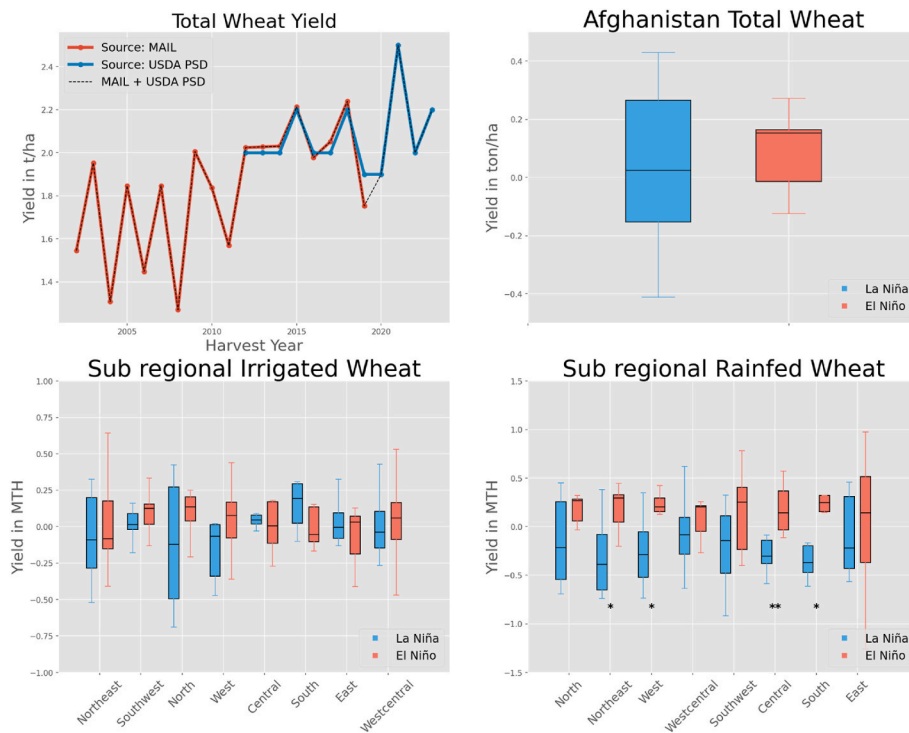


Fig. 11. Total wheat yield at national level as sourced by Afghanistan Ministry of Agriculture, Irrigation and Livestock (MAIL) and United States Department of Agriculture’s Foreign Agricultural Service’s Production Supply and Distribution (USDA PSD) (top left), composites of total wheat yield at national level for La Niña versus El Niño years during 2002–2019 period (top right), composites of wheat yield at sub-regional level for La Niña versus El Niño years during 2002–2019 period for irrigated wheat (bottom left) and for rainfed wheat (bottom right). The black line inside the box shows the median of each composite. The corresponding whisker caps display the values within 1.5 times the interquartile range at both ends. The order of the sub-regions in the case of irrigated and rainfed wheat is based on the order of the mean production for respective production reports over 2002–2019. * indicates statistical significance of difference in both composites at 90% confidence level, and ** indicates the same at 95% confidence level

Table 2

Excerpts from the FEWS NET reports focusing on agricultural production and food security conditions during the La Niña years listed above

La Niña events	Excerpts from FEWS NET food security report
2021/22	“At the national level, both rainfed and irrigated wheat production is likely to be below average, with northern and northeastern rainfed areas expected to experience the greatest deficits. Additionally, below-average snowfall during the 2021/22 wet season has led to below-average irrigation water availability. This will likely lead to below-average production of second season crops (including rice, maize, vegetables, and cash crops), with downstream areas worst affected.” (FEWS NET, 2022)
2020/21	“Conflict and poor agricultural production expected to drive deteriorating food security in Afghanistan” (FEWS NET 2021)
2017/18	“Drought, Conflict, and Displacement drive food insecurity across the country” (FEWS NET 2018)
2010/11	“The 2011 wheat harvest will leave a 2 million metric ton national deficit, with most crop losses occurring in rainfed areas in the north, central, and western provinces.” (FEWS NET 2011)
2007/08	“Below-average precipitation and early snowmelt during the 2007/08 winter season have led to below-average wheat production and pasture conditions. Labor migration, not typical for this time of year, is widespread, and access to drinking water is deteriorating.” “The impact of the current drought is most severe in areas which depend on rain-fed agriculture, rather than irrigation. Ninety percent of rain-fed wheat acreage has no yield while irrigated wheat yield is likely to decrease by 20–30 percent in areas of the northwest where farmers are faced with water shortages”. (FEWS NET, 2008)
2005/06	“Drought causes food and water shortages in the north”. “Inadequate and poorly distributed precipitation during the 2005/06 winter has resulted in a 50 percent loss of rain-fed cereal production in northern Afghanistan and caused severe water shortages.” (FEWS NET 2006)

4. Conclusion and discussion

Afghanistan is amongst the most food insecure countries in the world (GHI 2022). Drought is one of the several drivers of food insecurity. Past studies have examined the influence of ENSO on Central Asia, Southwest Asia climate and highlighted that La Niña is generally associated with higher chances of below average winter seasonal precipitation. However, several open questions regarding ENSO influence on drought in Afghanistan and variability in its influence in the country remained

In this study, using multiple indicators of different flavors of droughts – meteorological, hydrological, agricultural – as well as available wheat yield reports, we aim to answer the central question: What is the influence of ENSO on the drought outlook in Afghanistan and how does that influence vary spatially? To examine ENSO influence on drought outlook we compare the probability of drought indicators being in lower tercile during La Niña versus El Niño years. Application of multiple drought indicators and datasets is done to ensure that findings of this study are not specific to the choice of indicator or dataset. However, data quality can be inherently a potential source of uncertainties. Figs. S5 and S6a show the number of stations ingested in CHIRPS is low (varying from less than 10 to about 50) but consistent with lack of stations used in past studies focused on Afghanistan (Dost et al., 2023; Qutbudin et al., 2019; Shokory et al., 2023). Also as shown in Fig. S6, other gridded rainfall datasets that include in situ data such as GPCP (Schamm et al., 2014; Schneider et al., 2014, 2022) and APHRODITE (Yatagai et al., 2009) also face similar lack of in situ information in Afghanistan (Figs. S6b and S6c). CHIRPS, however, is not solely based on in situ rainfall reports and uses satellite-derived, infrared, temperature-based precipitation estimates as an input as well (Funk et al., 2015a). Nonetheless, we used three other precipitation datasets to examine the probability of SPI being in lower tercile during

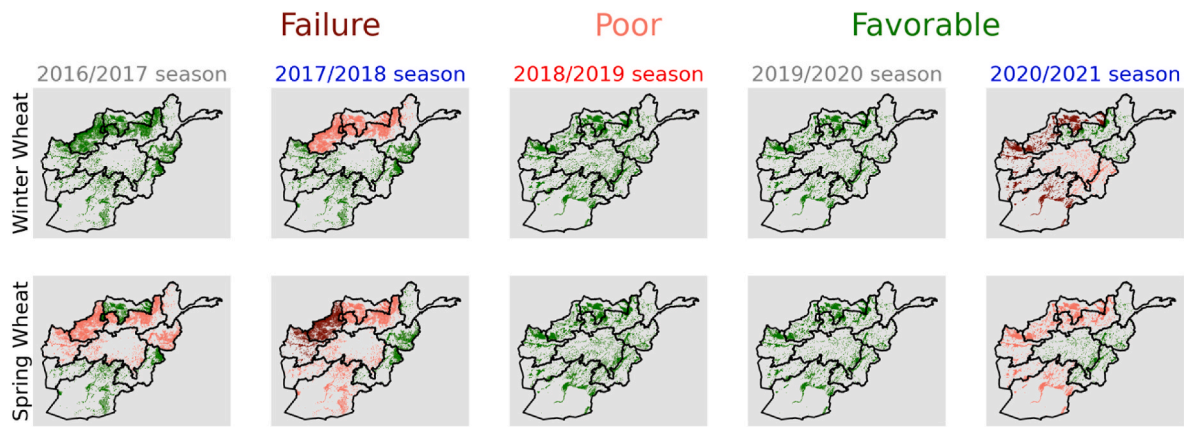


Fig. 12. End of season “Winter Wheat” (top panel) and “Spring Wheat” (bottom panel) crop conditions as reported by Crop Monitor for Early Warning (CM4EW) during 2016/2017 to 2020/2021 season. The crop conditions are classified as one of the three categories “Failure,” “Poor,” and “Favorable.” The font color of the season in the title for each year indicates if the year was a La Niña (blue color) or an El Niño (red color) year (For interpretation of the references to color in this figure legend, the reader is referred to the Web version of this article.)

ENSO events to compare with the results of section 4.1 (Fig. S7). Despite the differences in the mean seasonal precipitation (Fig. S8a) and standard deviation (Fig. S8b) amongst different datasets, all of the datasets indicate higher probability of SPI being in lower tercile during La Niña versus El Niño years (Fig. S7)

Similarly for snow drought we compared the results obtained using FLDAS JFM SWE (McNally et al. 2017; 2022) with ERA5-Land JFM SWE (Fang and Leung 2023; Gottlieb and Mankin 2024; Muñoz-Sabater et al. 2021; Tarek et al., 2020) and find the La Niña versus El Niño years diversity in the snow drought probability to be consistent in both datasets (Fig. S9), despite the differences in mean and standard deviation of JFM SWE among both datasets (Fig. S10). This study, however, does not account for glacier melts and its contribution to runoff, which can be particularly critical for Amu Darya and Kabul basins where most of the glaciers in Afghanistan reside and are reported to be declining since 1990s, due to a warming trend (Maharjan and Coauthors, 2021; Shokory et al., 2023)

Lastly, this study focuses exclusively on understanding ENSO’s impact on droughts in Afghanistan with the goal of leveraging the skillful long-lead ENSO forecasts (Ham et al., 2019; Lou et al., 2023) to provide a long-lead drought outlook in Afghanistan to support early warning of food insecurity. However, as the growing season approaches it is important to consider the impacts of other large scale climate oscillations and regional factors, which are known to modulate (amplify or dampen) ENSO’s impacts on subseasonal to seasonal climate in Afghanistan. These climate oscillations include North Atlantic Oscillation (Syed et al., 2006), Indian Ocean Dipole and West Pacific sea surface temperatures (Ashok and Saji 2007; Barlow et al., 2002) and Madden–Julian oscillation (Nazemosadat et al., 2023). Additionally, the teleconnections through east Pacific or central Pacific El Niño events are different (Alizadeh-Choobari 2017), and ENSO’s teleconnections are influenced by natural decadal variability and global warming (Alizadeh, 2022a, Alizadeh, 2024, Alizadeh, 2022b). This variability in ENSO’s teleconnection and influence of other climate oscillations warrant consideration in early warning of drought outlooks in Afghanistan

With the above caveats, the primary conclusions of the study are as follows

- (1) Probability of drought in Afghanistan substantially increases during La Niña years (often >50% and reaching >70% in some cases) particularly in North, Northeast, and West regions where probability of below normal, tends to be statistically significant, as per multiple indicators. Also, the probability of below normal drought during El Niño years is generally lower than 33%

- (2) La Niña years increase the probability of a snow drought in Afghanistan, with estimated average decrease in SWE volume over the five major basins in the country to be between 9% and 30%, with statistical significance in parts of Amu Darya basin which is the leading source of water resources in Afghanistan
- (3) La Niña also increased the probability of hydrologic drought with the probability of March–July (MAMJJ) simulated total runoff being below normal reaching >60% (particularly in the Harirod-Murghab, Helmand, and Kabul basins). MAMJJ total runoff volume is estimated to be reduced (on average) by 28%–42% in the 5 major basins in Afghanistan. It is also shown that mean WY water level as well as water level in the peak months, in the case of Kajaki reservoir, is generally lower during La Niña years (average standardized anomaly of ~ -0.6) versus El Niño years (average standardized anomaly of $+0.8$). In the available record, the two years with the lowest water level coincide with double La Niña (two La Niña in a row) years
- (4) La Niña also increases the probability of agricultural drought and decreases wheat yields mainly in rainfed regions but to a lesser extent in irrigated regions as well particularly in North, Northeast, and West sub-regions. The probability of April NDVI being below normal is found to be higher than 70% in the rainfed and irrigated areas of Northeast, North, and West regions. This result is at least partly supported by the wheat yield reports which may have data quality issues. Nonetheless, wheat yield composites for La Niña years tend to be lower than El Niño years for all reports of rainfed wheat and in some cases for irrigated wheat. The difference in La Niña and El Niño composites are not statistically significant for any of the irrigated wheat yield reports but are significant for Northeast (the second largest producer of rainfed wheat), West, and South regions at 90% confidence level and for the Central region at 95% confidence level

We also compared the main findings of this analysis with FEWS NET and CM4EW reports and found them to be generally in agreement, specifically La Niña years, in general, coincided with reports of drought and worsening food insecurity (FEWS NET reports) with some exceptions such as 2008–09 and 2011–12 seasons, and with “Failure” or “Poor” crop conditions as per CM4EW crop classification reports. However, we also acknowledge that some of the drought indicators used in this analysis were also considered in the reports by FEWS NET and CM4EW. For example, CHIRPS precipitation and eMODIS NDVI (now replaced with eVIIRS NDVI) often appear in those reports but those reports are also based on the expert judgments in the region and field reports (e.g. in situ data, as well as reports from key informants), and

additional inputs from multiple early warning systems and agencies (Becker-Reshef et al. 2020; Funk et al. 2019) thus they do not exclusively rely on the indicators used in this analysis. Additionally, some of the indicators used in this analysis become operational post 2015 (e.g. SPI, SPEI, FLDAS) so they were not used in the pre-2015 FEWS NET reports

Also, although we used several different indicators to examine the impacts of ENSO on seasonal droughts, a future study could also examine ENSO impacts on other important characteristics which can contribute to poor agricultural outcome and worsening of food insecurity, flooding, such as length of the rainy season, rain versus snow events, increase in number of hot and dry days, as well as the changes in timing of the reservoir filling, groundwater recharge. Nonetheless, the results of this study are directly applicable to early warning systems that focus on food security in the region. The findings indicate that in general, in a La Niña year, it is prudent to operate under the assumption that rainfed agricultural production particularly in North, Northeast, and West regions will be adversely affected and that some of the irrigated areas in those regions may experience production shortfall as well. Recent studies have shown a promising level of skill in long-term ENSO forecasts. For example, North American Multimodel Ensemble (NMME) models are shown to have skillful ENSO forecasts for up to 12 months in the future (Barnston et al., 2019; Tippett et al., 2019). Similarly, it is shown that with the application of deep learning methods, skillful ENSO forecasts can be made for up to 18–24 months in advance (Ham et al., 2019; Lou et al., 2023). Combined with these advances in ENSO forecasting and the knowledge of ENSO based drought and agriculture outcome outlook in Afghanistan, early warning agencies could be prepared for the development of food insecurity up to 1–2 years in advance

Lastly, the presented framework can be used for analyzing impacts of ENSO (or other multiyear climatic oscillations) on droughts in other climatically vulnerable regions using open-access datasets with global span. It is often the case that most climate-sensitive regions are also marked by a lack of in situ datasets either spatially or temporally and often leading to a greater need for reliance on global datasets such as those used in this study

CRedit authorship contribution statement

Shraddhanand Shukla: Writing – original draft, Visualization, Validation, Project administration, Methodology, Investigation, Funding acquisition, Formal analysis, Data curation, Conceptualization. **Fahim Zaheer:** Writing – review & editing, Data curation. **Andrew Hoell:** Writing – review & editing, Supervision, Methodology. **Weston Anderson:** Writing – review & editing, Methodology, Data curation. **Harikishan Jayanthi:** Writing – review & editing, Conceptualization. **Greg Husak:** Writing – review & editing, Funding acquisition, Data curation. **Donghoon Lee:** Writing – review & editing, Data curation. **Brian Barker:** Writing – review & editing, Data curation. **Shahriar Pervez:** Writing – review & editing, Data curation. **Kimberly Slinski:** Writing – review & editing, Data curation. **Christina Justice:** Writing – review & editing. **James Rowland:** Writing – review & editing, Funding acquisition, Data curation. **Amy L. McNally:** Writing – review & editing, Data curation. **Michael Budde:** Writing – review & editing, Resources, Funding acquisition. **James Verdin:** Writing – review & editing, Resources, Funding acquisition.

Declaration of competing interest

The authors declare the following financial interests/personal relationships which may be considered as potential competing interests: Shraddhanand Shukla reports financial support was provided by United States Geological Survey and by United States Agency for International Development. Weston Anderson, Kimberly Slinski, Amy L. McNally reports financial support was provided by United States Agency for International Development. Shahriar Pervez reports financial support was provided by United States Geological Survey.

Data availability

Data will be made available on request.

Acknowledgments

The FLDAS data used in this effort were acquired as part of the activities of NASA's Science Mission Directorate, and are archived and distributed by the Goddard Earth Sciences (GES) Data and Information Services Center (DISC). This work is supported by the U.S. Geological Survey, United States grant (#G21AC00026). HJ's work was performed under contract 140G0124D0001. AM, KS, WA were supported by the Bureau of Humanitarian Assistance, U.S. Agency for International Development, under the terms of NASA GSFC PAPA# AID-720BHAH00005 "Famine Early Warning Systems Network (FEWS NET)" and NASA Harvest Consortium (NASA Applied Sciences grant # 80 NSSC17K0625). This manuscript has been peer reviewed and approved for publication consistent with USGS Fundamental Science Practices (<https://pubs.usgs.gov/circ/1367/>). Any use of trade, firm, or product names is for descriptive purposes only and does not imply endorsement by the U.S. Government

Appendix A. Supplementary data

Supplementary data to this article can be found online at <https://doi.org/10.1016/j.wace.2024.100697>.

References

- Alami, M.M., Hayat, E., Tayfur, G., 2017. Proposing a popular method for meteorological drought monitoring in the Kabul river basin. *International Journal of Advanced Engineering Research and Science (IJAERS)* 4 (6). <https://doi.org/10.22161/ijaers.4.6.12>. Jun- 2017] ISSN: 2349-6495(P) | 2456-1908.
- Aliyar, Q., Zulfikar, F., Datta, A., Kuwornu, J.K.M., Shrestha, S., 2022. Drought perception and field-level adaptation strategies of farming households in drought-prone areas of Afghanistan. *Int. J. Disaster Risk Reduc.* 72, 102862 <https://doi.org/10.1016/j.ijdrr.2022.102862>.
- Alizadeh, O., 2022a. Amplitude, duration, variability, and seasonal frequency analysis of the El Niño-Southern Oscillation. *Clim. Change* 174, 20. <https://doi.org/10.1007/s10584-022-03440-w>.
- Alizadeh, O., 2022b. A review of the El Niño-southern oscillation in future. *Earth Sci. Rev.* 235, 104246 <https://doi.org/10.1016/j.earscirev.2022.104246>.
- Alizadeh, O., 2024. A review of ENSO teleconnections at present and under future global warming. *WIREs Clim. Change* 15, e861. <https://doi.org/10.1002/wcc.861>.
- Alizadeh-Choobari, O., 2017. Contrasting global teleconnection features of the eastern Pacific and central Pacific El Niño events. *Dynam. Atmos. Oceans* 80, 139–154. <https://doi.org/10.1016/j.dynatmoce.2017.10.004>.
- Alizadeh-Choobari, O., Adibi, P., 2019. Impacts of large-scale teleconnections on climate variability over Southwest Asia. *Dynam. Atmos. Oceans* 86, 41–51. <https://doi.org/10.1016/j.dynatmoce.2019.02.001>.
- Anderson, M.C., Hain, C., Wardlow, B., Pimstein, A., Mecikalski, J.R., Kustas, W.P., 2011. Evaluation of drought indices based on thermal remote sensing of evapotranspiration over the continental United States. *J. Clim.* 24, 2025–2044. <https://doi.org/10.1175/2010JCLI3812.1>.
- Ashok, K., Saji, N.H., 2007. On the impacts of ENSO and Indian Ocean dipole events on sub-regional Indian summer monsoon rainfall. *Nat. Hazards* 42, 273–285. <https://doi.org/10.1007/s11069-006-9091-0>.
- Barlow, M., Cullen, H., Lyon, B., 2002. Drought in central and Southwest Asia: La Niña, the warm pool, and Indian ocean precipitation. *J. Clim.* 15, 697–700. [https://doi.org/10.1175/1520-0442\(2002\)015<0697:DICASA>2.0.CO;2](https://doi.org/10.1175/1520-0442(2002)015<0697:DICASA>2.0.CO;2).
- Barlow, M., Cullen, H., Lyon, B., Hoell, A., Agel, L., 2021. An evaluation of CMIP6 historical simulations of the cold season teleconnection between tropical indo-pacific sea surface temperatures and precipitation in Southwest Asia, the coastal Middle East, and northern Pakistan and India. *J. Clim.* 34, 6905–6926. <https://doi.org/10.1175/JCLI-D-19-1026.1>.
- Barnston, A.G., Tippett, M.K., Ranganathan, M., L'Heureux, M.L., 2019. Deterministic skill of ENSO predictions from the North American Multimodel ensemble. *Clim. Dynam.* 53, 7215–7234. <https://doi.org/10.1007/s00382-017-3603-3>.
- Becker-Reshef, I., Coauthors, 2010. Monitoring global croplands with coarse resolution earth observations: the global agriculture monitoring (GLAM) project. *Rem. Sens.* 2, 1589–1609. <https://doi.org/10.3390/rs2061589>.
- Becker-Reshef, I., Coauthors, 2020. Strengthening agricultural decisions in countries at risk of food insecurity: the GEOGLAM Crop Monitor for Early Warning. *Remote Sens. Environ.* 237, 111553 <https://doi.org/10.1016/j.rse.2019.111553>.
- Bhattacharyya, K., Azizi, P.M., Shobair, S.S., Mohsini, M.Y., 2004. Drought impacts and potential for their mitigation in southern and western Afghanistan. In: *Working Paper, 91. Sri Lanka: International Water Management Institute, Colombo*.

- Brown, M.E., de Beurs, K.M., 2008. Evaluation of multi-sensor semi-arid crop season parameters based on NDVI and rainfall. *Remote Sens. Environ.* 112, 2261–2271. <https://doi.org/10.1016/j.rse.2007.10.008>.
- Chen, Y., Penton, D., Karim, F., Aryal, S., Wahid, S., Taylor, P., Cuddy, S.M., 2023. Characterisation of meteorological drought at sub-catchment scale in Afghanistan using station-observed climate data. *PLoS One* 18, e0280522. <https://doi.org/10.1371/journal.pone.0280522>.
- Dost, R., Kasiviswanathan, K.S., 2023. Quantification of water resource sustainability in response to drought risk assessment for Afghanistan river basins. *Nat. Resour. Res.* 32, 235–256. <https://doi.org/10.1007/s11053-022-10129-5>.
- Dost, R., Soundharajan, B.-S., Kasiviswanathan, K.S., Patidar, S., 2023. Quantifying drought characteristics in complex climate and scarce data regions of Afghanistan. *Geosciences* 13, 355. <https://doi.org/10.3390/geosciences13120355>.
- Fang, Y., Leung, L.R., 2023. Northern hemisphere snow drought in earth system model simulations and ERA5-land data in 1980–2014. *J. Geophys. Res. Atmospheres* 128, e2023JD039308. <https://doi.org/10.1029/2023JD039308>.
- FEWS NET, 2006. Afghanistan: food security warning - Afghanistan. Beyond Relief. <https://reliefweb.int/report/afghanistan/afghanistan-food-security-warning>. (Accessed 16 March 2023).
- FEWS NET, 2008. Executive overview of food security 28 May 2008 - Afghanistan. Beyond Relief, p. 1. <https://reliefweb.int/report/afghanistan/executive-overview-food-security-28-may-2008>. Accessed.
- FEWS NET, 2022. Afghanistan Key Message Update: rainfed crops and pasture significantly impacted by drought in north and northeast. May 2022 - Afghanistan | ReliefWeb, pp. 1–2. <https://reliefweb.int/report/afghanistan/afghanistan-key-message-update-rainfed-crops-and-pasture-significantly-impacted-drought-north-and-northeast-may-2022>. Accessed.
- FEWS NET, 2011. Afghanistan food security outlook july to december 2011 - Afghanistan | ReliefWeb. <https://reliefweb.int/report/afghanistan/afghanistan-food-security-outlook-july-december-2011>. (Accessed 16 March 2023).
- FEWS NET, 2018. Afghanistan food security outlook update, august 2018 - Afghanistan | ReliefWeb. <https://reliefweb.int/report/afghanistan/afghanistan-food-security-outlook-update-august-2018>. (Accessed 16 March 2023).
- FEWS NET, 2021. Afghanistan food security outlook, June 2021 to January 2022 - Afghanistan | ReliefWeb. <https://reliefweb.int/report/afghanistan/afghanistan-food-security-outlook-june-2021-january-2022>. (Accessed 16 March 2023).
- FEWS NET, 2023. Afghanistan - key message update: tue, 2023-01-10 | famine early warning systems Network. <https://fewsn.net/central-asia/afghanistan/key-message-update-january-2023>. (Accessed 9 March 2023).
- Funk, C., Budde, M.E., 2009. Phenologically-tuned MODIS NDVI-based production anomaly estimates for Zimbabwe. *Remote Sens. Environ.* 113, 115–125. <https://doi.org/10.1016/j.rse.2008.08.015>.
- Funk, C., Budde, M.E., Coauthors, 2015a. The climate hazards infrared precipitation with stations—a new environmental record for monitoring extremes. *Sci. Data* 2, 1–21. <https://doi.org/10.1038/sdata.2015.66>.
- Funk, C., Verdin, A., Michaelsen, J., Peterson, P., Pedreros, D., Husak, G., 2015b. A global satellite-assisted precipitation climatology. *Earth Syst. Sci. Data* 7, 275–287. <https://doi.org/10.5194/essd-7-275-2015>.
- Funk, C., Coauthors, 2019. Recognizing the famine early warning systems Network: over 30 Years of drought early warning science advances and partnerships promoting global food security. *Bull. Am. Meteorol. Soc.* 100, 1011–1027. <https://doi.org/10.1175/BAMS-D-17-0233.1>.
- Gelaro, R., Coauthors, 2017. The modern-era retrospective analysis for research and applications, version 2 (MERRA-2). *J. Clim.* 30, 5419–5454. <https://doi.org/10.1175/JCLI-D-16-0758.1>.
- GHI, 2022. Afghanistan. Glob. Hunger index GHI - peer-rev. Annu. Publ. Des. Comprehensively Meas. Track Hunger Glob. Reg. Ctry. Levels. <https://www.globalhungerindex.org/afghanistan.html>. (Accessed 9 February 2023).
- Goes, B.J.M., Howarth, S.E., Wardlaw, R.B., Hancock, I.R., Parajuli, U.N., 2016. Integrated water resources management in an insecure river basin: a case study of Helmand River Basin, Afghanistan. *Int. J. Water Resour. Dev.* 32, 3–25. <https://doi.org/10.1080/07900627.2015.1012661>.
- Gottlieb, A.R., Mankin, J.S., 2024. Evidence of human influence on Northern Hemisphere snow loss. *Nature* 625, 293–300. <https://doi.org/10.1038/s41586-023-06794-y>.
- Groten, S.M.E., 1993. NDVI—crop monitoring and early yield assessment of Burkina Faso. *Int. J. Rem. Sens.* 14, 1495–1515. <https://doi.org/10.1080/01431169308953983>.
- Ham, Y.-G., Kim, J.-H., Luo, J.-J., 2019. Deep learning for multi-year ENSO forecasts. *Nature* 573, 568–572. <https://doi.org/10.1038/s41586-019-1559-7>.
- Hobbins, M., Shukla, S., McNally, A., 2016. What role does evaporative demand play in driving drought in Africa? *Am. Geophys. Union*. <http://adsabs.harvard.edu/abs/2016AGUFMGC43F..02H>. (Accessed 3 July 2019).
- Hobbins, M., Shukla, S., McNally, A., Coauthors, 2023. A global long-term daily reanalysis of reference evapotranspiration for drought and food-security monitoring. *Sci. Data* 10, 746. <https://doi.org/10.1038/s41597-023-02648-4>.
- Hoell, A., Barlow, M., Saini, R., 2012. The leading pattern of intraseasonal and interannual Indian ocean precipitation variability and its relationship with asian circulation during the boreal cold season. *J. Clim.* 25, 7509–7526. <https://doi.org/10.1175/JCLI-D-11-00572.1>.
- Hoell, A., Barlow, M., Saini, R., Funk, C., Barlow, M., 2015a. The forcing of southwestern Asia teleconnections by low-frequency sea surface temperature variability during boreal winter. *J. Clim.* 28, 1511–1526. <https://doi.org/10.1175/JCLI-D-14-00344.1>.
- Hoell, A., Shukla, S., Barlow, M., Cannon, F., Kelley, C., Funk, C., 2015b. The forcing of monthly precipitation variability over Southwest Asia during the boreal cold season. *J. Clim.* 28, 7038–7056. <https://doi.org/10.1175/JCLI-D-14-00757.1>.
- Hoell, A., Barlow, M., Cannon, F., Xu, T., 2017. Oceanic origins of historical Southwest Asia precipitation during the boreal cold season. *J. Clim.* 30, 2885–2903. <https://doi.org/10.1175/JCLI-D-16-0519.1>.
- Hoell, A., Barlow, M., Xu, T., Zhang, T., 2018. Cold season Southwest Asia precipitation sensitivity to El Niño-southern oscillation events. *J. Clim.* 31, 4463–4482. <https://doi.org/10.1175/JCLI-D-17-0456.1>.
- Hoell, A., Eischeid, J., Barlow, M., McNally, A., 2020. Characteristics, precursors, and potential predictability of Amu Darya Drought in an Earth system model large ensemble. *Clim. Dynam.* 55, 2185–2206. <https://doi.org/10.1007/s00382-020-05381-5>.
- Huang, B., Coauthors, 2017. Extended reconstructed sea surface temperature, version 5 (ERSSTv5): upgrades, validations, and intercomparisons. *J. Clim.* 30, 8179–8205. <https://doi.org/10.1175/JCLI-D-16-0836.1>.
- Huang, X., Stevenson, S., 2023. Contributions of climate change and ENSO variability to future precipitation extremes over California. *Geophys. Res. Lett.* 50, e2023GL103322. <https://doi.org/10.1029/2023GL103322>.
- Husak, G.J., Michaelsen, J., Funk, C., 2007. Use of the gamma distribution to represent monthly rainfall in Africa for drought monitoring applications. *Int. J. Climatol.* 27, 935–944. <https://doi.org/10.1002/joc.1441>.
- IPC, 2022. IPC post-analysis monitoring brief september 2021 - January 2022. Food Security Cluster. <https://fscluster.org/afghanistan/document/ipc-post-analysis-monitoring-brief>. (Accessed 20 March 2023).
- Jenkerson, C.B., Maersperger, T., Schmidt, G., 2010. eMODIS: a user-friendly data source. U.S. Geological Survey. 2010-1055, viii, 10p. <http://pubs.er.usgs.gov/publication/ofr20101055>. Accessed.
- Lee, D., Coauthors, 2022. Maize yield forecasts for Sub-Saharan Africa using Earth Observation data and machine learning. *Global Food Secur.* 33, 100643. <https://doi.org/10.1016/j.gfs.2022.100643>.
- Lenssen, N.J.L., Goddard, L., Mason, S., 2020. Seasonal forecast skill of ENSO teleconnection maps. *Weather Forecast.* 35, 2387–2406. <https://doi.org/10.1175/WAF-D-19-0235.1>.
- Lou, J., Newman, M., Hoell, A., 2023. Multi-decadal variation of ENSO forecast skill since the late 1800s. *Npj Clim. Atmospheric Sci.* 6, 1–14. <https://doi.org/10.1038/s41612-023-00417-z>.
- Mariotti, A., 2007. How ENSO impacts precipitation in southwest central Asia. *Geophys. Res. Lett.* 34. <https://doi.org/10.1029/2007GL030078>.
- Mason, S.J., Goddard, L., 2001. Probabilistic precipitation anomalies associated with ENSO. *Bull. Am. Meteorol. Soc.* 82, 619–638. [https://doi.org/10.1175/1520-0477\(2001\)082<0619:PPAAWE>2.3.CO;2](https://doi.org/10.1175/1520-0477(2001)082<0619:PPAAWE>2.3.CO;2).
- McKee, T.B., Doesken, N.J., Kleist, J., 1993. The relationship of drought frequency and duration to time scales. 8th conference on applied climatology. In: 8th Conference on Applied Climatology. Anaheim, pp. 179–184.
- McNally, A., Coauthors, 2017. A land data assimilation system for sub-Saharan Africa food and water security applications. *Sci. Data* 4, 170012. <https://doi.org/10.1038/sdata.2017.12>.
- McNally, A., Coauthors, 2022. A Central Asia hydrologic monitoring dataset for food and water security applications in Afghanistan. *Earth Syst. Sci. Data* 14, 3115–3135. <https://doi.org/10.5194/essd-14-3115-2022>.
- Muhammad, A., Kumar Jha, S., Rasmussen, P.F., 2017. Drought characterization for a snow-dominated region of Afghanistan. *J. Hydrol. Eng.* 22, 05017014. [https://doi.org/10.1061/\(ASCE\)HE.1943-5584.0001543](https://doi.org/10.1061/(ASCE)HE.1943-5584.0001543).
- Muñoz-Sabater, J., Coauthors, 2021. ERA5-Land: a state-of-the-art global reanalysis dataset for land applications. *Earth Syst. Sci. Data* 13, 4349–4383. <https://doi.org/10.5194/essd-13-4349-2021>.
- Nabizada, A.F., Roustai, I., Dalvi, M., Olafsson, H., Siedliska, A., Baranowski, P., Krzyszczyk, J., 2022. Spatial and temporal assessment of remotely sensed land surface temperature variability in Afghanistan during 2000–2021. *Climate* 10, 111. <https://doi.org/10.3390/cli10070111>.
- Nazemosadat, M.J., Shahgholian, K., Ghaedamini, H., 2023. The wet and dry spells within the MJO-phase 8 and the role of ENSO and IOD on the modulation of these spells: a regional to continental-scales analysis. *Atmos. Res.* 285, 106631. <https://doi.org/10.1016/j.atmosres.2023.106631>.
- OCHA, 2023. Afghanistan humanitarian needs overview 2023 (January 2023) - Afghanistan. Beyond Relief. <https://reliefweb.int/report/afghanistan/afghanistan-humanitarian-needs-overview-2023-january-2023>. (Accessed 9 March 2023).
- Otkin, J.A., Svoboda, M., Hunt, E.D., Ford, T.W., Anderson, M.C., Hain, C., Basara, J.B., 2018. Flash droughts: a review and assessment of the challenges imposed by rapid-onset droughts in the United States. *Bull. Am. Meteorol. Soc.* 99, 911–919. <https://doi.org/10.1175/BAMS-D-17-0149.1>.
- Phillips, J.G., Cane, M.A., Rosenzweig, C., 1998. ENSO, seasonal rainfall patterns and simulated maize yield variability in Zimbabwe. *Agric. For. Meteorol.* 90, 39–50. [https://doi.org/10.1016/S0168-1923\(97\)00095-6](https://doi.org/10.1016/S0168-1923(97)00095-6).
- Qutbudin, I., Shiru, M.S., Sharafati, A., Ahmed, K., Al-Ansari, N., Yaseen, Z.M., Shahid, S., Wang, X., 2019. Seasonal drought pattern changes due to climate variability: case study in Afghanistan. *Water* 11, 1096. <https://doi.org/10.3390/w11051096>.
- Maharjan, S.B., Coauthors, 2021. Status and Decadal Changes of Glaciers in Afghanistan since 1990s. 2021. International Centre for Integrated Mountain Development (ICIMOD). <https://lib.icimod.org/record/35131> (Accessed on).
- Rout, B., 2008. How the water flows: a Typology of irrigation systems in Afghanistan. *Afghan. Res. Eval.* 1–80. Unit Issue Pap. Ser. <https://areu.org.af/publication/811/>. accessed on.
- Schamm, K., Ziese, M., Becker, A., Finger, P., Meyer-Christoffer, A., Schneider, U., Schröder, M., Stender, P., 2014. Global gridded precipitation over land: a description of the new GPCC First Guess Daily product. *Earth Syst. Sci. Data* 6, 49–60. <https://doi.org/10.5194/essd-6-49-2014>.

- Schneider, U., Becker, A., Finger, P., Meyer-Christoffer, A., Ziese, M., Rudolf, B., 2014. GPCP's new land surface precipitation climatology based on quality-controlled in situ data and its role in quantifying the global water cycle. *Theor. Appl. Climatol.* 115, 15–40. <https://doi.org/10.1007/s00704-013-0860-x>.
- Schneider, U., Hänsel, S., Finger, P., Rustemeier, E., Ziese, M., 2022. GPCP Climatology Version 2022 at 0.25°: Monthly Land-Surface Precipitation Climatology for Every Month and the Total Year from Rain-Gauges Built on GTS-Based and Historical Data. Globally Gridded Monthly Totals. min. 200 KByte-max. 10 MByte per gzip archive. https://doi.org/10.5676/DWD_GPCP/CLIM_M_V2022_025.
- Schwatke, C., Dettmering, D., Bosch, W., Seitz, F., 2015. Dahiti – an innovative approach for estimating water level time series over inland waters using multi-mission satellite altimetry. *Hydrol. Earth Syst. Sci.* 19, 4345–4364. <https://doi.org/10.5194/hess-19-4345-2015>.
- Sengupta, S., 2021. A New Breed of Crisis: War and Warming Collide in Afghanistan. *The New York Times*, August 30. <https://www.nytimes.com/2021/08/30/climate/afghanistan-climate-taliban.html>. Accessed on.
- Shahriar Pervez, M.S, Budde, M., Rowland, J., 2014. Mapping irrigated areas in Afghanistan over the past decade using MODIS NDVI. *Remote Sens. Environ.* 149, 155–165. <https://doi.org/10.1016/j.rse.2014.04.008>.
- Shahzaman, M., Coauthors, 2021. Remote sensing indices for spatial monitoring of agricultural drought in South Asian countries. *Rem. Sens.* 13, 2059. <https://doi.org/10.3390/rs13112059>.
- Shokory, J.A.N., Schaeffli, B., Lane, S.N., 2023. Water resources of Afghanistan and related hazards under rapid climate warming: a review. *Hydrol. Sci. J.* 68, 507–525. <https://doi.org/10.1080/02626667.2022.2159411>.
- Shukla, S., Husak, G., Turner, W., Davenport, F., Funk, C., Harrison, L., Krell, N., 2021. A slow rainy season onset is a reliable harbinger of drought in most food insecure regions in Sub-Saharan Africa. *PLoS One* 16, e0242883. <https://doi.org/10.1371/journal.pone.0242883>.
- Skakun, S., Justice, C.O., Vermote, E., Roger, J.-C., 2018. Transitioning from MODIS to VIIRS: an analysis of inter-consistency of NDVI data sets for agricultural monitoring. *Int. J. Rem. Sens.* 39, 971–992. <https://doi.org/10.1080/01431161.2017.1395970>.
- Syed, F.S., Giorgi, F., Pal, J.S., King, M.P., 2006. Effect of remote forcings on the winter precipitation of central southwest Asia part 1: observations. *Theor. Appl. Climatol.* 86, 147–160. <https://doi.org/10.1007/s00704-005-0217-1>.
- Tarek, M., Brisette, F.P., Arsenault, R., 2020. Evaluation of the ERA5 reanalysis as a potential reference dataset for hydrological modelling over North America. *Hydrol. Earth Syst. Sci.* 24, 2527–2544. <https://doi.org/10.5194/hess-24-2527-2020>.
- Tayfur, G., Alami, M.M., 2022. Meteorological drought analysis for Helmand river basin, Afghanistan. *Tek. Dergi* 33, 12223–12242. <https://doi.org/10.18400/tekderg.868595>.
- Tippett, M.K., Ranganathan, M., L'Heureux, M., Barnston, A.G., DelSole, T., 2019. Assessing probabilistic predictions of ENSO phase and intensity from the North American Multimodel Ensemble. *Clim. Dynam.* 53, 7497–7518. <https://doi.org/10.1007/s00382-017-3721-y>.
- Vicente-Serrano, S.M., Beguería, S., López-Moreno, J.I., 2010. A multiscalar drought index sensitive to global warming: the standardized precipitation evapotranspiration index. *J. Clim.* 23, 1696–1718. <https://doi.org/10.1175/2009JCLI2909.1>.
- WFP, and UNEP, 2018. Climate change in Afghanistan. In: What Does it Mean for Rural Livelihoods and Food Security? UNEP - UN Environ. Programme. <http://www.unep.org/resources/report/climate-change-afghanistan-what-does-it-mean-rural-livelihoods-and-food-security>. (Accessed 9 March 2023).
- Wiesmann, D., Biesalski, H., von Grebner, K., Bernstein, J., 2015. Methodological review and revision of the global hunger index. <https://doi.org/10.2139/ssrn.2673491>.
- Wilks, D.S., 2011. *Statistical Methods in the Atmospheric Sciences*. Academic Press, p. 698.
- Yang, Y., Coauthors, 2018. Field-scale mapping of evaporative stress indicators of crop yield: an application over Mead, NE, USA. *Remote Sens. Environ.* 210, 387–402. <https://doi.org/10.1016/j.rse.2018.02.020>.
- Yatagai, A., Arakawa, O., Kamiguchi, K., Kawamoto, H., Nodzu, M.I., Hamada, A., 2009. A 44-year daily gridded precipitation dataset for Asia based on a dense Network of rain gauges. *Inside Solaris* 5, 137–140. <https://doi.org/10.2151/sola.2009-035>.